1969

Longitudinal optical phonon-plasmon coupling in ionic semiconductors

Thomas Joseph McMahon

Department: Physics

LONGITUDINAL OPTICAL PHONON-PLASMON COUPLING IN IONIC SEMICONDUCTORS

by

THOMAS JOSEPH MCMAHON, 1943

A DISSERTATION 541

Presented to the Faculty of the Graduate School of the

UNIVERSITY OF MISSOURI - ROLLA

In Partial Fulfillment of the Requirements for the Degree

DOCTOR OF PHILOSOPHY

in

PHYSICS

1969

Robert J. Bell
Advisor

Wayne E. Tefft

Roland A. Hultsch

Robert Pearson

J. K. Foote

Otto L. Hill

W. F. Parks

LONGITUDINAL OPTICAL PHONON-PLASMON COUPLING IN IONIC SEMICONDUCTORS

An Abstract of a Dissertation

Presented to

the Faculty of the Graduate School

University of Missouri at Rolla

In Partial Fulfillment

of the Requirements for the Degree

Doctor of Philosophy

---

by

Thomas Joseph McMahon

1969

Abstract

The coupling of free carriers and lattice vibrational modes is studied in CdS and InSb by room temperature far infrared reflectance measurements. When the free carrier concentration is such that the plasma frequency is at or near the longitudinal optical mode frequency it is shown that while the transverse modes remain fixed, the longitudinal modes mix with the plasma mode and are shifted in a manner similar to that described by Varga in 1965. Using the dielectric function for the coupled system permits the determination of electron effective masses by reflectance measurements with lattice effects excluded. This method allows one to investigate the frequency shifts and effective mass values on crystals in which the mobility varies by more than an order of magnitude as demonstrated by the analysis of both CdS and InSb. In the case of CdS where the polaron coupling constant is large enough to have noticeable effects, account is taken of the polaron mass and of the additional absorption in the plasma mode at frequencies above the longitudinal optical phonon frequency.

ACKNOWLEDGMENTS

This investigation would not have been possible had it not been for the advice and support of Dr. Robert J. Bell as it was his idea to study this phenomenon and the experience I gained from him to actually carry out the infrared measurements.

I am also grateful for the financial support of the U. S. Bureau of Mines and the encouragement of Dr. Leroy Furlong.

The assistance of Mr. Kenneth Mustain and Joseph Blea with the vacuum spectrometer and the help of Alan Cobb and Jack Benoist with the computer programming were appreciated.

Mr. Fred Taylor's Hall measurement contributed directly.

TABLE OF CONTENTS

LIST OF ILLUSTRATIONS

Figures

Table

CHAPTER I

INTRODUCTION

The subject of this thesis is the coupling of free carriers and lattice vibrational modes in polar semiconductors which is most apparent when the concentration is such that the plasma frequency, ω_P, is at or near the longitudinal optical mode frequency, ω_L. The dielectric function for the coupled system of plasma and phonon modes was examined by infrared reflectance from surfaces of suitably doped single crystals. This dielectric function was derived by Varga[1] and expanded upon by Singwi and Tosi,[2] but it had been assumed and empirically used earlier by Collins and Kleinman[3] in the reflectance of ZnO in the long wavelength limit.

Measurement of the room temperature reflectance of a Ga doped single crystal of CdS was made with the electric vector parallel and perpendicular to the c-axis. The concentration of free electrons ($N = 1.32 \times 10^{18}$ cm^{-3}), as measured on a Hall bar taken from the reflectance sample, fixed ω_P at $1.12\omega_L$. The principal transverse optical mode frequency, ω_T, defines ω_L by the Lyddane-Sachs-Teller relation

$$\omega_L = [1 + \delta\varepsilon/\varepsilon_\infty]^{\frac{1}{2}} \omega_T ,$$

when damping and weaker modes are neglected.[4] Here $\delta\varepsilon$ is the principal mode strength and ε_∞ is the high frequency dielectric constant. In all cases the angle of incidence was 30 degrees and the data were analyzed using this value.

Polarized reflectances of two Te doped single crystals of InSb were made in which the free electron concentrations of $N = 1.43 \times 10^{17}$ cm^{-3} and 3.96×10^{17} cm^{-3} fixed ω_P at $0.85\omega_L$ and $1.41\omega_L$, respectively. Most of the effective mass variation with N in InSb that had been discussed by Spitzer and Fan[5] can be explained in terms of this coupling.

The validity of Varga's dielectric function has been substantiated through Raman scattering in n-type GaAs by the work of Mooradian and Wright,[6] Mooradian and McWhorter,[7] and Tell and Martin.[8] They have verified the longitudinal optical mode frequency shifts and in some cases the lifetimes.

A comparison of the lifetime as calculated from the Hall mobility is made with the plasma lifetime in the Drude free electron term of the dielectric function. In CdS, which has a polaron coupling constant[9] with a value of 0.58, the effect of an additional polaron mode absorption is very noticeable at frequencies just greater than ω_L as calculated by Gurevich, et al.[10] Analysis of the polaron effective mass is made in the same weak coupling approximation,[9] and with no additional parameters the fit of the reflectance data is greatly improved. Polaron effects were considered negligible in InSb as the coupling constant has a smaller value of 0.034.

A reflectance minimum relation has been derived[11] and is found to work quite well when applied to these and other doped samples of ZnO,[3] InSb,[5] GaAs,[12,13] and CdS.[14]

CHAPTER II

EXPERIMENTAL PROCEDURES

The experimental reflectance values are calculated by taking the ratios of sample reflected fluxes and the fluxes obtained by replacing the sample with an evaporated aluminum mirror (assumed to be 100% reflecting). For energies greater than 210 cm^{-1} a Beckman IR-12 was used in double beam operation with the reflectance attachment fixing the angle of incidence at 30 degrees. Wire grid polarizers,[15] purchased from the Perkin Elmer Corporation, were placed at the entrance slit to the grating section where no depolarization would occur between the samples and the polarizer. A substrate of AgCl was used for energies greater than 450 cm^{-1} and a polyethylene substrate for energies less than 450 cm^{-1}.

For energies less than 210 cm^{-1}, a single beam vacuum (used here at 150 x 10^{-3} torr) spectrometer, with a high pressure GE UA-2 mercury vapor lamp[16] as a source, was used. Elimination of visible and near infrared radiation was accomplished by scattering from a rough aluminum surface and transmission through black polyethylene[17] and crystalline quartz.[18] One piece of 0.006 inch thick black polyethylene was at room temperature and another 0.007 inch thick was at 4.2K located at the detector. One piece of crystal quartz 1/16 inch thick was at room temperature and two pieces each a millimeter thick were at 4.2K located at the detector. The light was chopped at 10 cycles per second by a semidisc blade

and detected by a Texas Instruments Ga doped germanium bolometer[19,20] operated at 4.2K. The band pass regions before the echellette gratings, used in a Czerny-Turner geometry, were further narrowed as shown in Table 1. The relative grating efficiencies for the various harmonics were also considered in narrowing these bands.

TABLE 1

Filtering for various energy regions in cm^{-1}.

Reflectance filters	100-125	125-155	155-210
220 rough Al surface	X	X	X
KBr crystal[21]		X	
Grating blazed at	$100cm^{-1}$	$166cm^{-1}$	$166cm^{-1}$
Transmission filters			
Black polyethylene 300K	X	X	X
½mm fused quartz[22] 300K	X		
1/16" crystal quartz 300K	X	X	X
Black polyethylene 4.2K	X	X	X
(2)1mm crystal quartz 4.2K	X	X	X

The samples were placed at a 60-degree angle in the brass light pipe and the angle of incidence was assumed to be 30 degrees. The wire grid polarizer was placed in a 4mm gap[23] as close to the sample as possible (½ inch) to reduce the amount of depolarization.

The Ga doped CdS crystal was purchased from the Clevite Corporation with the Hall bar cut directly from the center

of the polished face. The c-axis was parallel to the surface of the reflection sample and in the plane of incidence with polarization determined by rotating the polarizer. Room temperature Hall measurements showed a concentration of n-type carriers at 1.32×10^{18} cm^{-3} with a resistivity of 1.37×10^{-14} stat Ω-cm.

The Te doped InSb samples A and B were supplied by the Monsanto Company with Hall measurements showing free electron concentrations of 1.43×10^{17} cm^{-3} and 3.96×10^{17} cm^{-3}. The resistivities were 0.058×10^{-14} stat Ω-cm and 0.041×10^{-14} stat Ω-cm, respectively. The (111) planes were in the polished faces and π-polarizations were used rather than no polarization to allow the possibility of an exact calculation.

CHAPTER III

LONG WAVELENGTH DIELECTRIC FUNCTION

A derivation of the dielectric function for the coupled system of lattice vibrations and free carriers involves the following two assumptions.[1] First, only the lattice polarization contributes to the Lorentz field correction of the local electric field $\overline{E}^{i}_{loc}$ at the ion site in the i^{th} normal mode. Second, the free carriers feel only the macroscopic field $\overline{E}$ in the crystal since the carriers are characterized by a screening length larger than a lattice constant, i.e. there is no local field correction for the free carriers.

The first assumption means that for the i^{th} mode,

$$\overline{E}^{i}_{loc} = \overline{E} + \frac{4\pi}{3}\overline{P}^{i}_{lat} , \tag{1}$$

where $\frac{4\pi}{3}\overline{P}^{i}_{lat}$ is the Lorentz field correction due to the lattice polarization in the i^{th} mode $\overline{P}^{i}_{lat}$.

The second assumption means that the equation of motion for the free carriers is

$$m^{*}\frac{d^{2}}{dt^{2}}\overline{r}^{i} + (m^{*}/\tau^{i})\frac{d}{dt}\overline{r}^{i} = e^{i}\overline{E} , \tag{2}$$

where $\overline{r}^{i}$ is the position of the i^{th} carrier of charge e^{i} and effective mass m^{*} having an average collision lifetime τ^{i}. Assuming only one type of free carrier (electrons), then where there are N per unit volume

$$\bar{P}_{el} = \bar{P}_{el}(\bar{E}) - \bar{P}_{el}(\bar{0}) = \sum_{i=1}^{N} -e[\bar{r}^i(\bar{E}) - \bar{r}^i(\bar{0})] \qquad (3)$$

is the free electron contribution to the polarization due to $\bar{E}$. For each Fourier component the time dependence is assumed to be

$$\bar{E}(t) = \bar{E}_0 e^{-i\omega t} \qquad (4)$$

and upon substitution in (2),

$$\bar{r}^i(\bar{E}) = \frac{e\bar{E}(t)}{m^*(\omega^2 + i\omega/\tau)} \qquad (5)$$

With a uniform background of donor ions one takes the origin such that $\bar{P}_{el}(\bar{0})$ vanishes and obtains

$$\bar{P}_{el} = \frac{-Ne^2\bar{E}(t)}{m^*(\omega^2 + i\omega/\tau)} \quad . \qquad (6)$$

Consideration of the lattice composed of two types of ions follows much as in Born and Huang.[24] Let $\bar{u}_{\pm}^i$, $\pm Ze$, $\alpha_{\pm}^i$, and $M_{\pm}$ be respectively the displacements from equilibrium, the charges, the ionic polarizabilities, and the masses of the positive and negative ions in the i^{th} mode. Since there are $1/v$ ions per unit volume (v being the volume per ion pair), the polarization due to the i^{th} mode is

$$\bar{P}_{lat}^{\,i} = \frac{1}{v}[Ze(\bar{u}_+^i - \bar{u}_-^i) + (\alpha_+^i + \alpha_-^i)\bar{E}_{loc}^{\,i}]$$

$$= \frac{1}{v}[Ze(\bar{u}_+^i - \bar{u}_-^i) + (\alpha_+^i + \alpha_-^i)(\bar{E} + \tfrac{4\pi}{3}\bar{P}_{lat}^{\,i})] \qquad (7)$$

where the first term is due to the relative displacement

of the ions and the second term is the contribution from the ionic deformation and then

$$\bar{P}^{i}_{lat} = \frac{1}{v}[Ze(\bar{u}^{i}_{+} + \bar{u}^{i}_{-}) + \bar{E}(\alpha^{i}_{+} + \alpha^{i}_{-})]/[1 - \frac{4\pi}{3v}(\alpha^{i}_{+} + \alpha^{i}_{-})] \quad . \quad (8)$$

Considering only nearest neighbor interactions, the equations of motion for each type of ion in the i^{th} mode are

$$M_{+} \frac{d^2}{dt^2}\bar{u}^{i}_{+} + M_{+}\Gamma^{i}\frac{d}{dt}\bar{u}^{i}_{+} + K^{i}(\bar{u}^{i}_{+} - \bar{u}^{i}_{-}) = Ze\bar{E}^{i}_{loc} \quad (9)$$

and

$$M_{-} \frac{d^2}{dt^2}\bar{u}^{i}_{-} + M_{-}\Gamma^{i}\frac{d}{dt}\bar{u}^{i}_{-} + K^{i}(\bar{u}^{i}_{-} - \bar{u}^{i}_{+}) = -Ze\bar{E}^{i}_{loc} \quad , \quad (10)$$

where Γ^{i} is the velocity dependent damping parameter and K^{i} is the harmonic force constant acting on each ion. Multiplying (9) by M_{-}, (10) by M_{+}, subtracting, and defining the reduced mass of the ion pair $\mu = M_{+}M_{-}/(M_{+}+M_{-})$ results in

$$(\mu \frac{d^2}{dt^2} + \mu\Gamma^{i}\frac{d}{dt} + K^{i})(\bar{u}^{i}_{+} - \bar{u}^{i}_{-}) = Ze\bar{E}^{i}_{loc} \quad . \quad (11)$$

For a given Fourier component with $\bar{u}^{i}_{+}$, $\bar{u}^{i}_{-}$, and $\bar{E}^{i}_{loc}$ in phase

$$(-\omega^2 - i\omega\Gamma^{i} + K^{i}/\mu)(\bar{u}^{i}_{+} - \bar{u}^{i}_{-}) = Ze\bar{E}^{i}_{loc}/\mu \quad . \quad (12)$$

Substituting (1) and (8) into (12) results in

$$(-\omega^2 - i\omega\Gamma^{i} + \frac{K^{i}}{\mu} - \frac{4\pi Z^2e^2/3\mu v}{1-\frac{4\pi}{3v}(\alpha^{i}_{+}+\alpha^{i}_{-})})(\bar{u}^{i}_{+} - \bar{u}^{i}_{-}) = \frac{Ze\bar{E}/\mu}{1-\frac{4\pi}{3v}(\alpha^{i}_{+} + \alpha^{i}_{-})} \quad , \quad (13)$$

which leads to a more familiar form if the natural frequency of the i^{th} optic mode (shown later to be the i^{th} transverse optic mode frequency in Section 5) is defined to be

$$\omega_0^i = \{ \frac{K^i}{\mu} - \frac{4\pi Z^2 e^2/3\mu v}{1-\frac{4\pi}{3v}(\alpha_+^i+\alpha_-^i)} \}^{\frac{1}{2}} . \qquad (14)$$

At this point it is worth noting that the natural frequency of the i^{th} optic mode is not only dependent upon the harmonic force K^i but is softened by the ionic deformation of its neighbors.

The response function for the lattice becomes

$$\bar{u}_+^i - \bar{u}_-^i = \{\frac{Ze\bar{E}/\mu}{1-\frac{4\pi}{3v}(\alpha_+^i+\alpha_-^i)}\} / \{ \omega_0^{i\,2} - \omega^2 - i\omega\Gamma^i \} . \qquad (15)$$

For convenience the strength of the i^{th} mode is defined by

$$\delta\varepsilon^i = \frac{4\pi Z^2 e^2/\mu v\omega_0^{i\,2}}{[1-\frac{4\pi}{3v}(\alpha_+^i+\alpha_-^i)]^2} \qquad (16)$$

and when (15) and (16) are substituted into (3)

$$\bar{P}_{lat}^{\,i} = \frac{[4\pi\delta\varepsilon^i]\,\bar{E}}{1-(\omega/\omega_0^i)^2-i\omega\Gamma^i/\omega_0^{i\,2}} - \frac{[\alpha_+^i+\alpha_-^i]\,\bar{E}}{v[1-\frac{4\pi}{3v}(\alpha_+^i+\alpha_-^i)]} . \qquad (17)$$

The total polarization is

$$\bar{P}_{tot} = \sum_{\substack{\text{optic}\\ \text{modes}}} \bar{P}_{lat}^{\,i} + \bar{P}_{el} , \qquad (18)$$

where the sum over the optic modes is taken at points where the wave vector is nearly zero. The long wavelength approximation was imposed by the fact that no spatial variation was considered in dealing with $\bar{E}$. This is a valid limit to take in the analysis to be done since the wavelength of the far infrared for consideration is at least 10^3 times longer

than a lattice constant. So in the definition of the dielectric function for a principal axis direction

$$\varepsilon(0,\omega) = 1 + 4\pi P_{tot}(0,\omega)/E \quad , \tag{19}$$

the '0' indicates that the wave vector is nearly zero. The dielectric function in terms of basic parameters is

$$\varepsilon(0,\omega) = 1 + \sum_{\text{modes}} \frac{\delta\varepsilon^i}{1-(\omega/\omega_0^i)^2 - i\omega\Gamma^i/\omega_0^{i\,2}} + \frac{4\pi(\alpha_+^i + \alpha_-^i)}{v[1-\frac{4\pi}{3v}(\alpha_+^i+\alpha_-^i)]} - \frac{4\pi Ne^2}{m^*(\omega^2+i\omega/\tau)} \quad . \tag{20}$$

Usually for experimental purposes (20) may be simplified by defining the high frequency and the clamped dielectric constants for the pure ionic crystal (N=0) respectively as

$$\varepsilon_\infty = \lim_{\omega\to\infty} \varepsilon(0,\omega) \quad \text{and} \quad \varepsilon_0 = \lim_{\omega\to 0} \varepsilon(0,\omega) \quad . \tag{21}$$

The final generalized form of the dielectric function describing an ionic lattice with several optic modes and with free carriers is then

$$\varepsilon(0,\omega) = \varepsilon_\infty - \frac{4\pi Ne^2}{m^*(\omega^2+i\omega/\tau)} + \sum_{\text{modes}} \frac{\delta\varepsilon^i}{1-(\omega/\omega_0^i)^2 - i\omega\Gamma^i/\omega_0^{i\,2}} \tag{22}$$

A useful relation to note is

$$\varepsilon_0 = \varepsilon_\infty + \sum_{\text{modes}} \delta\varepsilon^i \quad . \tag{23}$$

CHAPTER IV

ANALYSIS

The analysis was approached by relating the real and imaginary parts of $\varepsilon(0,\omega)$, expressed by Eq. (22), to the complex index of refraction, $n_c = n + i\kappa$, by the use of

$$n_c n_c = \varepsilon(0,\omega)$$

which leads to

$$n^2 - \kappa^2 = \mathrm{Re}[\varepsilon(0,\omega)]$$

and (24)

$$2n\kappa = \mathrm{Im}[\varepsilon(0,\omega)] \quad .$$

In making the best fit of the reflectance data, ε_∞, $\delta\varepsilon^i$, ω_0^i, Γ^i, m^*, and τ were treated as parameters. The concentration, N, was found from the corresponding Hall measurement.

The values of n and κ depend upon the principal axis direction chosen for ε by the orientation of the electric field with respect to the crystal axes. Since the electric field has already been restricted to a principal axis direcion by Eq. (19), the analysis of the reflection from CdS could be carried out easily with a slight modification of the equations of Mosteller and Wooten[25] for the reflection from uniaxial absorbing crystals at oblique incidence. The modification was made entirely by a geometrical consideration in the following way.

Geometry of ref. 25.

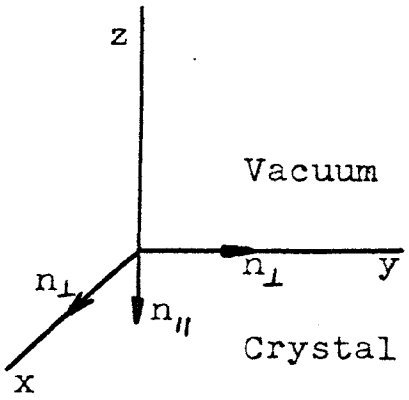

Geometry for CdS crystal.

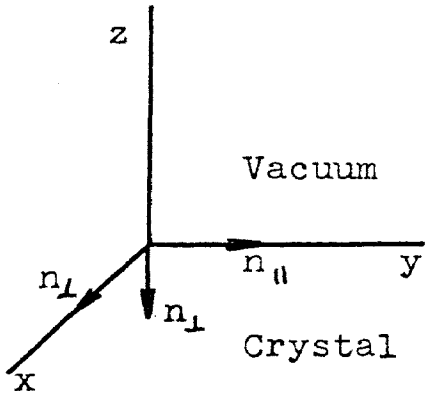

Fig. 1. Optic axis orientation.

In Fig. 1 the plane of incidence for either geometry is defined by the y-z plane and the surface of reflection is the x-y plane. In the geometry of ref. 25 the c-axis (the unique direction) of the uniaxial crystal is along the z-direction perpendicular to the surface as indicated by the index symbol $n_{||}$. However, to make the analysis sensitive to both principal axes, the c-axis of the CdS crystal was chosen to be in the surface and in the plane of incidence, i.e. along the y-axis. The index of refraction for the direction perpendicular to the c-axis is indicated by $n_\perp$.

In the σ-configuration (electric vector perpendicular to the plane of incidence) the reflectance is identical for either geometry and is given by

$$R_\sigma = [(\cos\theta - a)^2 + b^2]/[(\cos\theta + a)^2 + b^2] \qquad (25)$$

where

$$2\left(\frac{a^2}{b^2}\right) = [(n_\perp^2-\kappa_\perp^2-\sin^2\theta)^2+4n_\perp^2\kappa_\perp^2]^{\frac{1}{2}} \pm (n_\perp^2-\kappa_\perp^2-\sin^2\theta) .$$

In order that the expression for the reflectance in the

π-configuration (electric vector in the plane of incidence) of Ref. 25 be applied to the geometry of the CdS sample, $n_\perp$ and $n_{||}$ as well as $\kappa_{||}$ and $\kappa_\perp$ must be interchanged in the expression for R_π as they are in Fig. 1. The expression for the modified relation is therefore

$$R_\pi = \frac{(c\cos\theta - a)^2 + (d\cos\theta - b)^2}{(c\cos\theta + a)^2 + (d\cos\theta + b)^2} \qquad (26)$$

where

$$c = n_\perp n_{||} - \kappa_\perp \kappa_{||}$$

and

$$d = n_\perp \kappa_{||} + n_{||} \kappa_\perp \ .$$

The InSb samples were analysed in the π-configuration by noting $n_{||} = n_\perp$ and $\kappa_{||} = \kappa_\perp$ and using the R_π relation.

CHAPTER V

NORMAL MODES

The normal modes of a system of free carriers and phonons in the long wavelength limit may be found in the following two ways. The first way is mentioned and referenced because the term coupling the plasma to the phonons is explicitly used in determining the normal modes. In the second way the coupling is not explicit but the method is more applicable for any experimental analysis.

In the first way Singwi and Tosi[2] represent the Hamiltonian for the coupled system in diagonal form except for the element connecting the longitudinal optic mode coordinate with the plasma mode coordinate. This interaction element depends only upon the plasma and longitudinal optic modes as in this model these are the only sources of electric fields and it is given by Born and Huang[24] as

$$H_{int} = -\omega_L \left[\frac{1}{4\pi}(1/\epsilon_\infty - 1/\epsilon_0) \right]^{\frac{1}{2}} \int (\bar{u}_+ - \bar{u}_-)_{long} \cdot \bar{E}_{el} d^3r \ ,$$

where

$$\bar{E}_{el}(r,t) = \text{grad} \int -\rho(\bar{r}',t)/(\bar{r}-\bar{r}') \ d^3r' \ .$$

Here $(\bar{u}_+ - \bar{u}_-)_{long}$ is the relative displacement of the positive and negative ions along the propagation vector and $\rho(\bar{r}',t)$ is the free carrier charge density at the point $\bar{r}'$. The diagonalization procedure[2] results in the longitudinal

optic mode frequencies

$$(\omega_{\pm})^2 = \tfrac{1}{2}(\omega_L^2+\omega_P^2) \pm \tfrac{1}{2}[(\omega_L^2-\omega_P^2)^2 + 4\omega_L^2\omega_P^2(1-\varepsilon_\infty/\varepsilon_0)]^{\frac{1}{2}} \quad (27)$$

where $\omega_P^2=4\pi Ne^2/m^*\varepsilon_\infty$ is the classical plasma frequency squared. The transverse normal mode frequencies remain unchanged as they have no electric field to couple with the plasma.

While this method is appealing from a theoretical viewpoint, it becomes awkward to use in a real situation where finite phonon and plasmon lifetimes exist.

The second way makes direct use of the dielectric function derived in Chapter 3. Following a standard calculation as presented by Barker,[4] one notes that by a suitable arrangement of charge and current sources, waves of arbitrary wave vector, $\bar{k}$, and frequency may be excited. However, to find the free vibrations of a crystal the following form of Maxwell's equations must be satisfied to remove sources of free currents and charges from the medium.

$$\text{div } \bar{D} = \text{div } \bar{H} = 0 , \quad \text{curl } \bar{E} = -\frac{\partial \bar{H}}{\partial ct} ,$$

and

$$\text{curl } \bar{H} = \frac{\partial \bar{D}}{\partial(ct)} , \text{ with } \quad \bar{D} = \varepsilon\bar{E}$$

for a principal axis direction. The longitudinal and transverse solutions are separated by considering the first of these relations, that is

$$\text{div } \bar{D} = \varepsilon \text{ div } \bar{E} = 0 .$$

If the div $\overline{E} = 0$, then ε need not be zero for a plane wave with $\overline{k}$ perpendicular to $\overline{E}$ (a transverse wave); but if $\varepsilon = 0$, then $\overline{k}$ turns out to be parallel to $\overline{E}$ (a longitudinal wave)[24]. The longitudinal solutions are then defined as being those frequencies at which $\mathrm{Re}[\varepsilon(0,\omega)]$ vanish. The transverse solutions are found by the elimination of $\overline{H}$ from the two curl relations and applying the transversality condition $\overline{k}\cdot\overline{E} = 0$ which results in

$$(ck/\omega)^2 = \varepsilon(0,\omega) \quad . \tag{28}$$

In a dispersion plot the solutions to this equation show that it is a result of the mixing of a pure radiation field and a pure transverse lattice mode. These mixed photon-phonon modes are referred to as polariton modes and their existence has been varified by the Raman work of Henry and Hopfield[26] in GaP. This effect can be used to explain the shape of the reflectance curve for a single mode crystal without free carriers as shown in Chapter VIII.

For most purposes it is adequate to neglect the variation of the transverse solution with $\overline{k}$ and define the i^{th} solution as the position of the i^{th} pole in the complex plane of $\varepsilon(0,\omega)$, given by

$$\omega_T^i = \pm(\omega_0^{i\,2} - \Gamma^{i\,2}/4)^{\frac{1}{2}} - i\Gamma^i/2 \ ,$$

which for most cases may be approximated as

$$\omega_T^i \simeq \omega_0^i \ , \quad \text{for} \quad \Gamma^i << \omega_0^i \ . \tag{29}$$

With these conventions to be followed from here on, the simplest case of one phonon and one plasma mode will be discussed as it may be applied to the cases where there is one mode whose $\delta\varepsilon$ is much greater than any of the others and where there is one predominant free carrier. Then Eq. (22) becomes

$$\varepsilon(0,\omega) = \varepsilon_\infty + \frac{\delta\varepsilon}{1-(\omega/\omega_0)^2-i\omega\Gamma/\omega_0^2} - \frac{4\pi Ne^2}{m^*(\omega^2+i\omega/\tau)} \quad .$$

When N=0 and if $\omega_0 >> \Gamma$, Eq. (29) is valid and the Lyddane-Sachs-Teller relation[27] follows directly as

$$\omega_L^2/\omega_T^2 = \varepsilon_0/\varepsilon_\infty \quad . \tag{30}$$

where ε_0, the low frequency dielectric constant, is $\varepsilon_\infty + \delta\varepsilon$. With these considerations the mixed longitudinal mode frequencies (frequencies at which $\mathrm{Re}[\varepsilon(0,\omega)]$ vanish) are

$$\omega_\pm^2 = \tfrac{1}{2}(\omega_L^2+\omega_P^2) \pm \tfrac{1}{2}[(\omega_L^2+\omega_P^2)^2 - 4\omega_L^2\omega_P^2\varepsilon_\infty/\varepsilon_0]^{\frac{1}{2}} \tag{31}$$

which may be shown to be the same mode frequencies expressed by Eq. (27). For an arbitrary material the normal mode frequencies as a function of concentration in the reduced units $\omega_P^2/\omega_L^2 = 4\pi Ne^2/m^*\varepsilon_\infty\omega_L^2$ are shown in Fig. 2.

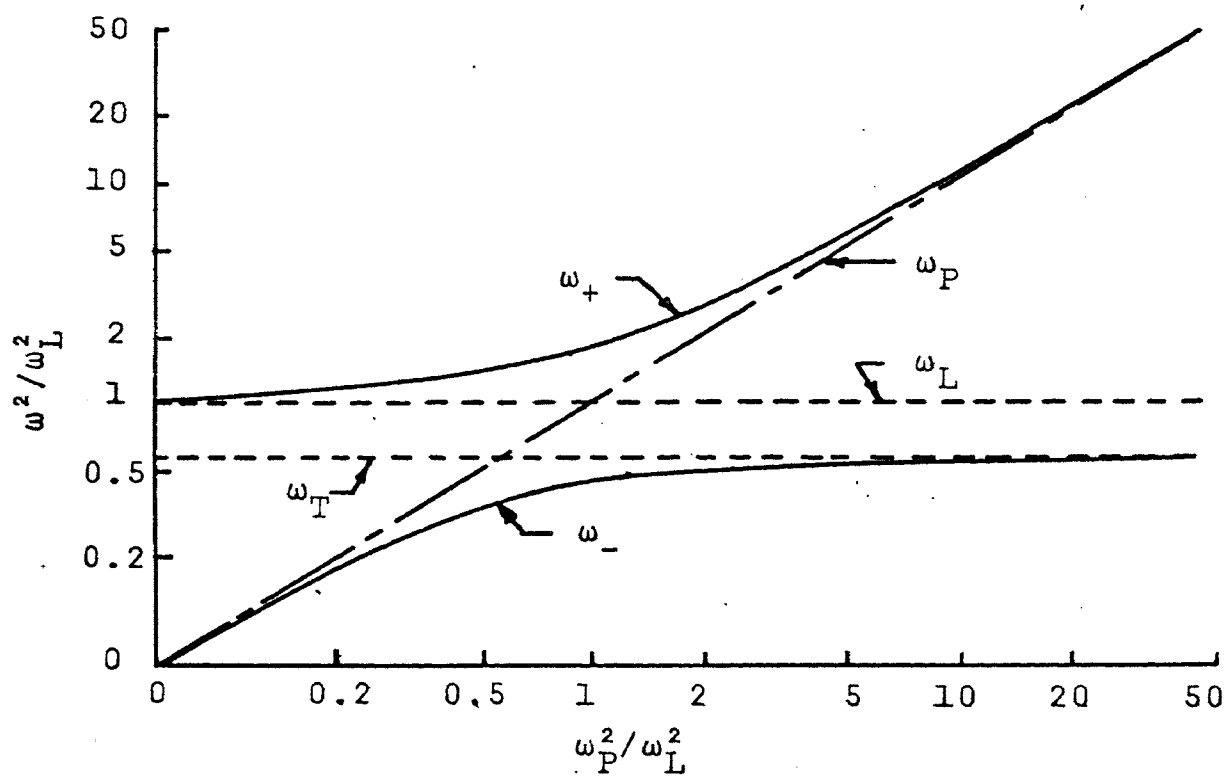

Fig. 2. Normal mode frequencies as a function of concentration.

This plot demonstrates qualitatively the coupling of the plasma mode and longitudinal optic mode particularly in the region where ω_P is near ω_L. It is here that the actual longitudinal modes take on a mixed character which is typical of coupled systems where the crossing of modes is avoided. The lower branch at small concentrations is plasmon-like becoming mixed with increasing concentration as described above. With very large concentrations the lower branch takes on a pure phonon character as it approaches the transverse optic mode. The upper branch has complete phonon character for small concentrations and results in a pure plasma mode with very large carrier concentrations.

The transverse mode is fixed as it has no associated

electric field. It is the same electric field associated with the longitudinal optic mode coupling it to the free carriers that provides the additional restoring force to raise ω_L above ω_T.[28] Without this field the forces pulling the ions back to the equilibrium position would be identical for either mode in the long wavelength limit.[29]

CHAPTER VI

RESULTS

Reflectances of the InSb samples A and B in Figs. 3 and 4 were fit by assuming the Hall values of $N = 1.43 \times 10^{17}$ cm^{-3} and 3.96×10^{17} cm^{-3}, respectively, and $\varepsilon_\infty = 15.68$[30] and then adjusting ω_0, $\delta\varepsilon$, Γ, m^*, and τ to obtain the best fit. The values of ω_0 and $\delta\varepsilon$ were in agreement with the values found for pure InSb[31]. This indicates no shift in the transverse mode frequency. The value of Γ in these doped samples was 3 to 4 times that found for the pure InSb.[31] The free electrons showed effective masses $m^* = 0.030m_e$ and $0.031m_e$ in samples A and B, respectively. These values are not as low as and do not vary as much as would be predicted if the lattice were not included in the dielectric function as in Ref. 5. The data of Ref. 5 indicate a more rapid decrease in effective mass with smaller concentrations because the minimum analysed, which is attributed to the plasma edge at higher concentrations, becomes a result of the coupled plasma-phonon system as ω_P nears ω_L. In the reflectance minima discussion of Chapter VIII, a value of $m^* = 0.030m_e$ was used in the theory to fit the minimum frequencies of Ref. 5 and the data taken on samples A and B.

In sample A (or sample B) the Drude relaxation time made at optical frequencies, $\tau_{opt} = 5.4 \times 10^{-13}$ sec (or 3.3×10^{-13}

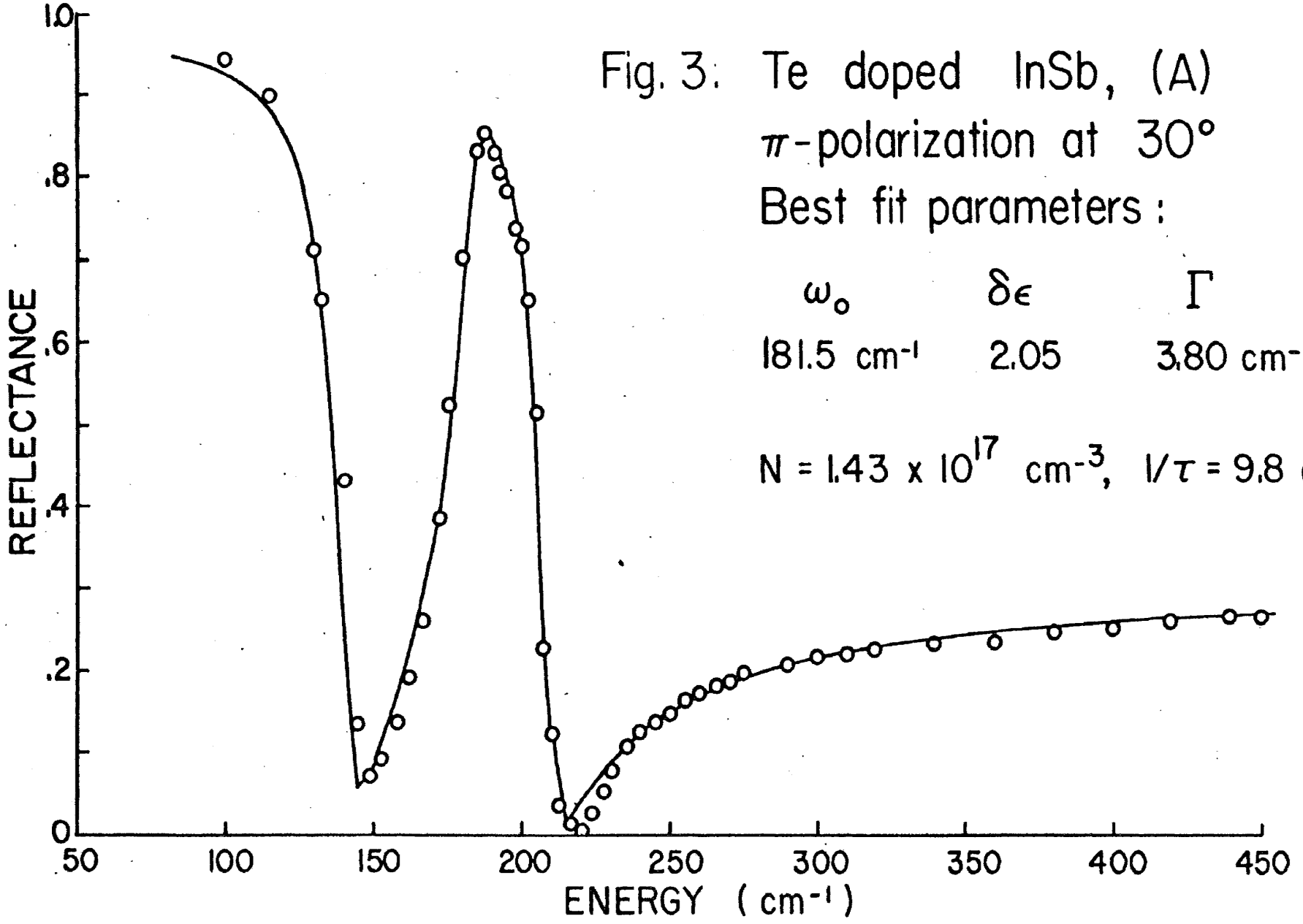

Fig. 3: Te doped InSb, (A) π-polarization at 30°
Best fit parameters :

ω_o	$\delta\epsilon$	Γ
181.5 cm^{-1}	2.05	3.80 cm^{-1}

$N = 1.43 \times 10^{17}$ cm^{-3}, $1/\tau = 9.8$ cm^{-1}

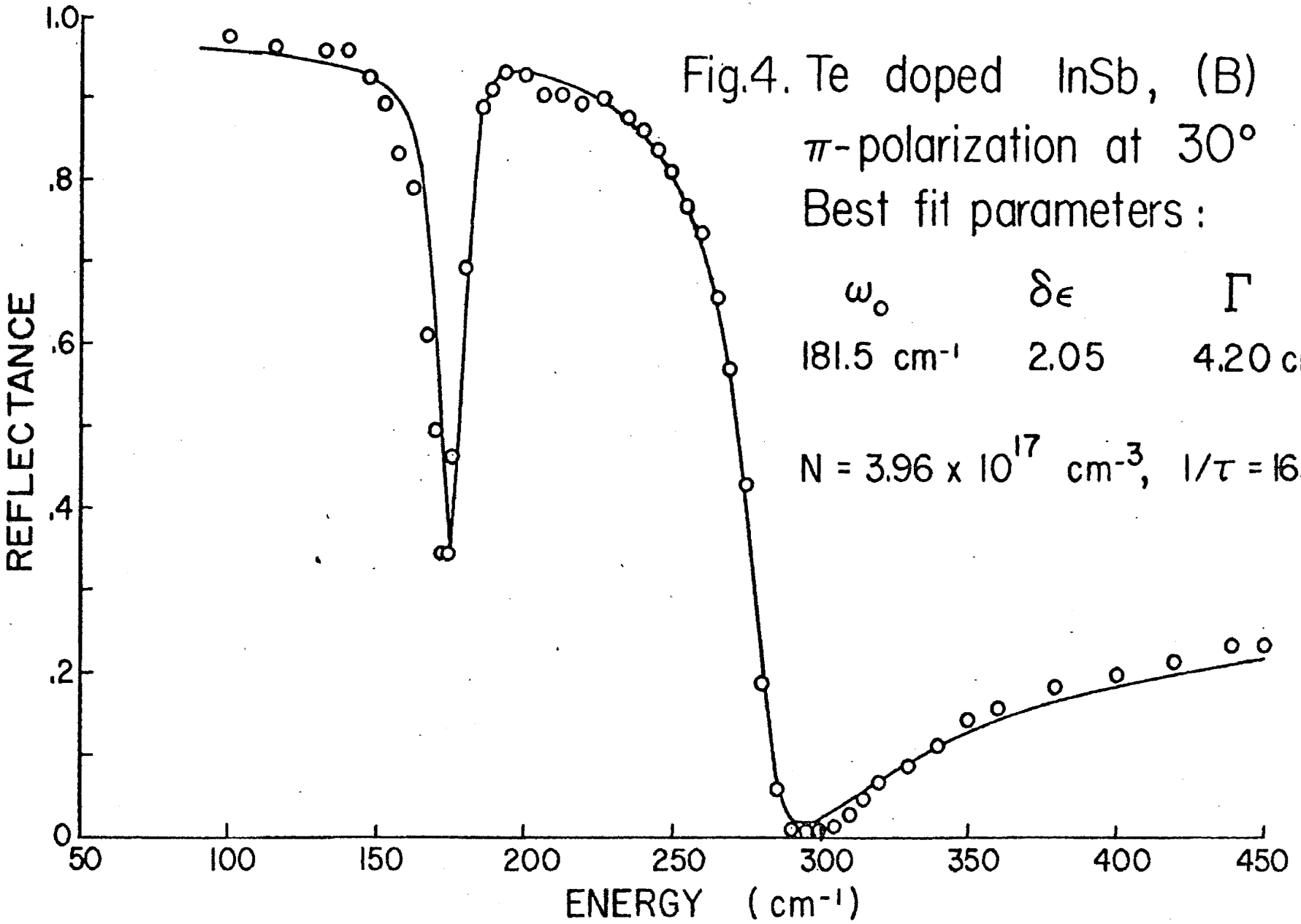

Fig.4. Te doped InSb, (B) π-polarization at 30°
Best fit parameters:

ω_o	$\delta\epsilon$	Γ
181.5 cm^{-1}	2.05	4.20 cm^{-1}

$N = 3.96 \times 10^{17}$ cm^{-3}, $1/\tau = 16.2$ cm^{-1}

sec), is a little less than the values obtained by a static Hall measurement, $\tau_H = m^*/\rho Ne^2 = 6.6 \times 10^{-13}$ sec (or 3.4×10^{-13} sec). From the reflectance fits, values of τ_{opt} could be determined with a 5 percent accuracy and values of m^* could be more accurately determined to about 2 percent.

Figs. 5 and 6 show the data for the CdS sample measured in both polarizations which were normalized in the range of the IR-12 at 1950 cm^{-1} to the dielectric constant parallel to the c-axis, $\varepsilon_\infty^\pi = 5.17$,[32] and perpendicular to the c-axis, $\varepsilon_\infty^\sigma = 5.23$,[32] because part of the surface was not polished well. The reflectances taken in the 100 cm^{-1} to 210 cm^{-1} range were again direct ratios with values obtained from the aluminum mirror. The lattice parameters compare well with the values found for pure CdS[33] in both polarizations with the exception of Γ^1 for the main peak of the reflectance curve in the π-polarization. Using the Hall value for $N = 1.32 \times 10^{18}$ cm^{-3}, the effective mass is found to be $m^* = 0.20m_e$ from the best fit in agreement with others.[34,35] The fit to the reflectance data is poor in the 300 cm^{-1} to 600 cm^{-1} range and could not be improved without destroying the fit elsewhere. Further consideration of this will be made in Chapter VII.

For CdS the optical value of $\tau_{opt} = 2.1 \times 10^{-14}$ sec is again smaller than the value $\tau_H = 4.3 \times 10^{-14}$ sec obtained from a static Hall measurement.

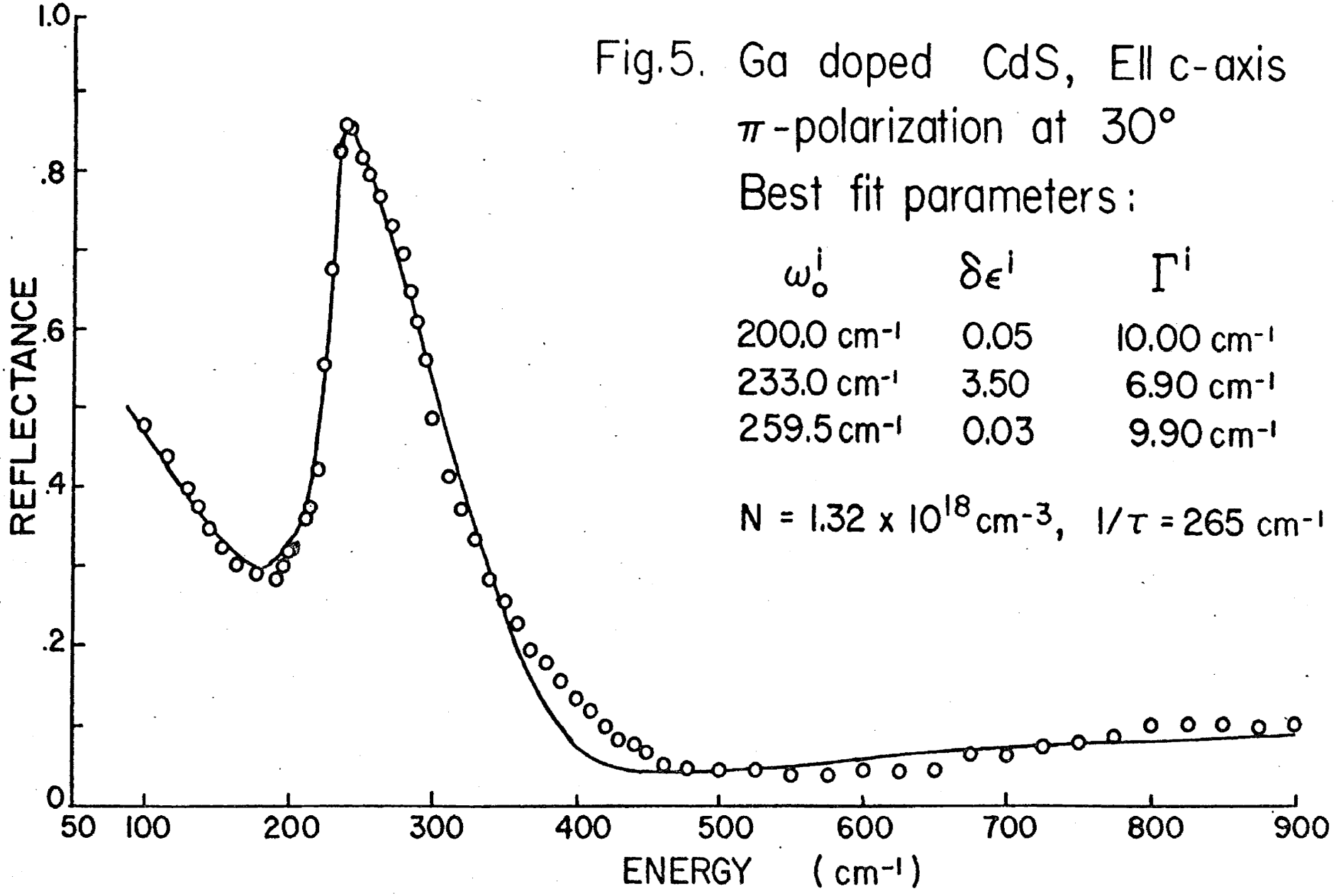

Fig.5. Ga doped CdS, E∥ c-axis
π-polarization at 30°
Best fit parameters:

ω_o^i	$\delta\epsilon^i$	Γ^i
200.0 cm^{-1}	0.05	10.00 cm^{-1}
233.0 cm^{-1}	3.50	6.90 cm^{-1}
259.5 cm^{-1}	0.03	9.90 cm^{-1}

$N = 1.32 \times 10^{18} cm^{-3}$, $1/\tau = 265\ cm^{-1}$

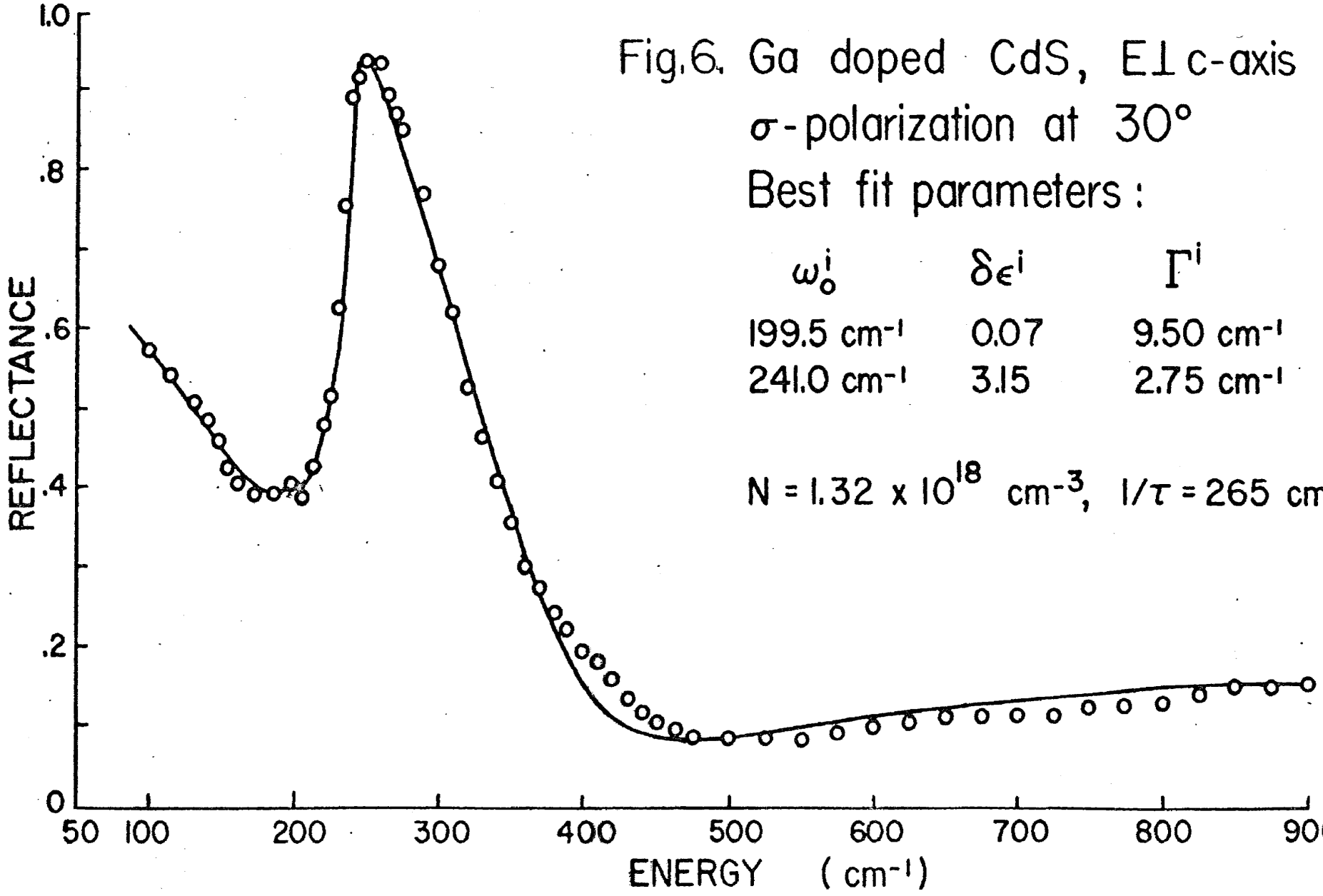

Fig. 6. Ga doped CdS, E⊥c-axis
σ-polarization at 30°
Best fit parameters :

ω_o^i	$\delta\epsilon^i$	Γ^i
199.5 cm^{-1}	0.07	9.50 cm^{-1}
241.0 cm^{-1}	3.15	2.75 cm^{-1}

$N = 1.32 \times 10^{18}$ cm^{-3}, $1/\tau = 265$ cm^{-1}

Though the transverse mode frequencies are unshifted, the longitudinal mode frequencies, i.e., those frequencies at which the real part of the dielectric function vanish when the imaginary part is small, are shifted in the manner described by Varga.[1] As an example, the real and imaginary parts of the dielectric function calculated from the best fit of the data shown in Fig. 6 are shown in Fig. 7. The coupled longitudinal mode frequencies expressed by Eq. (31),

$$\omega_{\pm}^2 = \tfrac{1}{2}(\omega_L^2+\omega_P^2) \pm \tfrac{1}{2}[(\omega_L^2+\omega_P^2)^2 - 4\omega_L^2\omega_P^2\varepsilon_\infty/\varepsilon_0]^{\frac{1}{2}} \qquad (31)$$

in this CdS crystal would be calculated at $\omega_+ = 410$ cm^{-1} and $\omega_- = 210$ cm^{-1}. Instead, as shown in Fig. 7, they occur at the much lower values of 374 cm^{-1} and 13 cm^{-1} because the imaginary part of the dielectric function is not small, particularly in the region of the lower normal mode frequency.

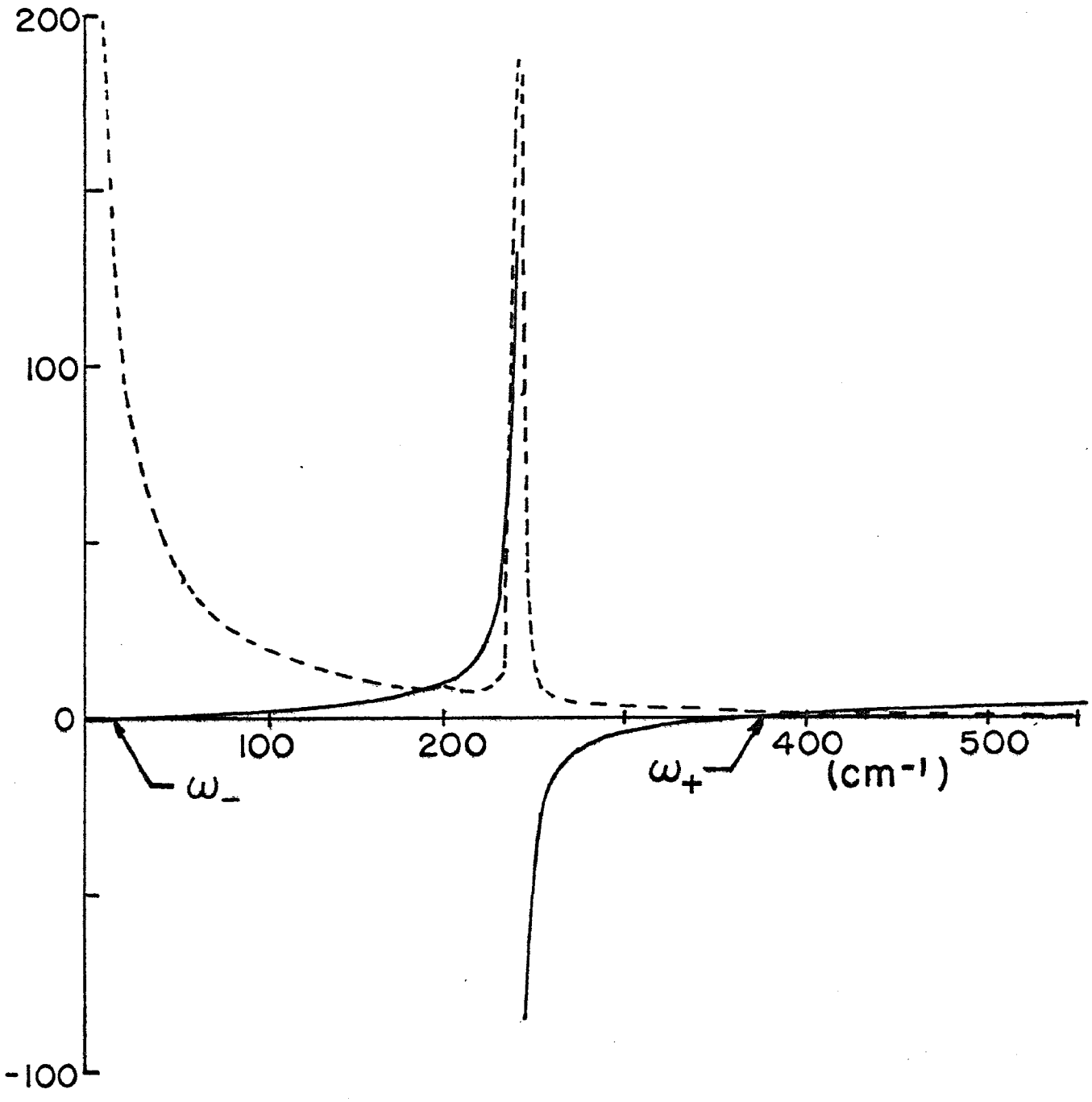

Fig. 7. The real (————) and imaginary (------) parts of the dielectric function calculated from the best reflection fit in Fig. 6 for Ga doped CdS.

CHAPTER VII

POLARON MASS AND ABSORPTION

Two corrections to the dielectric function expressed by Eq. (22) will be considered here. First, a slow electron (one whose primary interaction with the lattice polarization occurs through coulomb forces) moving through a polar crystal displaces the positive and negative ions with respect to one another. The effect of the polarization field on the motion of the electron can be accounted for in a modification of its effective mass. In this derivation there is no frequency dependence assumed for the motion of the electron, and the electron with its associated polarization field is called a polaron. Its mass is called a polaron mass and will be denoted by m_p.

As in this work the motions in time vary at infrared frequencies, the polaron mass will be used only when the frequency of the driving field is less than the longitudinal optic mode frequency. This will be assumed because at frequencies greater than ω_L the inertia of this mode is too large for its polarization to respond to the electron's motion. At frequencies greater than ω_L the effective mass m^* as used previously remains.

The calculation exhibited here was done by Fröhlich[9] and follows from the point at which the Hamiltonian for the

electron-phonon system has been derived in Ref. 9 as

$$H = \frac{p_e^2}{2m^*} + \int \{\frac{\gamma}{2}[\frac{d\bar{P}_{ir}}{dt}^2 + \omega_L^2 \bar{P}_{ir}^2] - \bar{D}(r,r_e)\cdot\bar{P}_{ir}(r)\}\, d^3r \quad , \qquad (32)$$

where $\bar{p}_e$ is the electron's momentum, $\bar{P}_{ir}(r)$ is the polarization due to the relative displacement of the positive and negative ions in the longitudinal optic mode, $\bar{D}(r,r_e)$ is the displacement field from the electron at r_e and is given by $-e\,grad[1/(r-r_e)]$, and $(1/\gamma) = (\omega_L^2/4\pi)(1/\varepsilon_\infty - 1/\varepsilon_0)$.

Since the interaction of $\bar{P}_{ir}(r)$ with the magnetic field of a slow electron is negligible compared to the electrostatic interaction, the irrotational condition

$$curl\ \bar{P}_{ir}(r) = 0 \qquad (33)$$

may be imposed. One may then assume that $\bar{P}_{ir}(r)$ is derivable from the potential $\Phi_{ir}(r)$ through the relation

$$4\pi\bar{P}_{ir}(r) = grad\ \Phi_{ir}(r) \quad . \qquad (34)$$

The interaction term in Eq. (32) for an electron with the lattice polarization can be simplified in the following way with the use of Green's Theorem

$$-\int \bar{D}(r,r_e)\cdot\bar{P}_{ir}(r)\, d^3r = \frac{1}{4\pi}\int [grad(\frac{e}{r-r_e})]\cdot[grad\ \Phi_{ir}(r)]d^3r$$

$$= e\ \Phi_{ir}(r) \quad . \qquad (35)$$

The actual calculation is simplified some by the use of the complex field operators

$$\bar{B}(r) = (\gamma\omega_L/2\hbar)^{\frac{1}{2}}[\bar{P}_{ir}(r) + \frac{i}{\omega_L}\frac{d}{dt}\bar{P}_{ir}(r)]$$

and (36)

$$\bar{B}^+(r) = (\gamma\omega_L/2\hbar)^{\frac{1}{2}}[\bar{P}_{ir}(r) - \frac{i}{\omega_L}\frac{d}{dt}\bar{P}_{ir}(r)] \quad .$$

The Hamiltonian given by Eq. (32) becomes

$$H=\frac{p_e^2}{2m^*}+\hbar\omega_L\int\bar{B}^+(r)\cdot\bar{B}(r)d^3r -(\frac{\hbar}{2\gamma\omega_L})^{\frac{1}{2}}\int\bar{D}(r,r_e)\cdot[\bar{B}^+(r)+\bar{B}(r)]d^3r \quad . \quad (37)$$

When periodic boundary conditions over a cube of volume $V=L^3$ are assumed, the field operators may be written as

$$\bar{B}(r) = \sum_{\bar{w}}(\bar{w}/wV^{\frac{1}{2}})\ e^{i\bar{w}\cdot\bar{r}}b_{\bar{w}} \text{ and } \bar{B}^+(r) = \sum_{\bar{w}}(\bar{w}/wV^{\frac{1}{2}})\ e^{-i\bar{w}\cdot\bar{r}}b^+_{\bar{w}} \quad (38)$$

where the components of the wave vector $\bar{w}$ satisfy

$$w_i = (2\pi/L)\ n_i \quad ; \quad n_i = 0, \pm1, \pm2, \ldots \quad . \quad (39)$$

Here $b_{\bar{w}}$ and $b^+_{\bar{w}}$ are the annihilation and creation operators, respectively, which either take away or add a longitudinal optic phonon of wave vector $\bar{w}$ to the total polarization field. As indicated by Eq. (36) with the substitution of Eq. (38), the total polarization field, $\bar{P}_{ir}(r)$, is a sum over all the phonon states described by these operators. These operators obey the commutation relations dictated by Bose statistics. Their properties and eigenstates are the same as those for the harmonic oscillator and are to be assumed without explanation.

Noting

$$\int \bar{B}^{+}(r)\cdot\bar{B}(r)d^{3}r = \frac{1}{V}\int \sum_{\bar{w}}(\bar{w}/w)e^{-i\bar{w}\cdot\bar{r}}b_{\bar{w}}^{+}\cdot\sum_{\bar{w}'}(\bar{w}'/w')e^{i\bar{w}'\cdot\bar{r}}b_{\bar{w}'}d^{3}r$$

$$= \frac{1}{V}\sum_{\bar{w},\bar{w}'} b_{\bar{w}}^{+}b_{\bar{w}'}(\bar{w}\cdot\bar{w}'/ww')\int e^{i(\bar{w}'-\bar{w})\cdot\bar{r}}\, d^{3}r$$

$$= \sum_{\bar{w}} b_{\bar{w}}^{+}b_{\bar{w}}\ \delta_{\bar{w},\bar{w}'} \qquad (40)$$

and using Eqs. (34), (35), (36), (38), and (40) in Eq. (37) yields

$$H = \frac{p_e^2}{2m^*} + \hbar\omega_L\sum_{\bar{w}} b_{\bar{w}}^{+}b_{\bar{w}} + i4\pi\left(\frac{e^2\hbar}{2\gamma V\omega_L}\right)^{\frac{1}{2}}\sum_{\bar{w}}\frac{1}{w}\left(b_{\bar{w}}^{+}e^{-i\bar{w}\cdot\bar{r}}e - b_{\bar{w}}e^{i\bar{w}\cdot\bar{r}}e\right). \qquad (41)$$

For convenience the polaron coupling constant, α, is introduced as

$$\alpha \equiv \frac{2\pi e^2 u}{\hbar\gamma(\omega_L)^3} = \tfrac{1}{2}(1/\varepsilon_\infty - 1/\varepsilon_0)\frac{e^2u}{\hbar\omega_L} \qquad (42)$$

where

$$(1/u) \equiv (\hbar/2m^*\omega_L)^{\frac{1}{2}} \quad . \qquad (43)$$

Expression (43) has been shown by Lee, Low, and Pines[36] to be the spatial extent of the polarization cloud associated with the electron and in CdS the calculated value is 10^{-7} cm. For CdS the polaron coupling constant is 0.58 and for InSb it is 0.034.

Defining the dimensionless quantities

$$\bar{x} = u\bar{r}_e \quad , \qquad \bar{v} = u^{-1}\bar{w} \quad , \text{ and} \quad S = Vu^3 \qquad (44)$$

the expression for H in units of $\hbar\omega_L$ becomes

$$F = -\sum_{i=1}^{3} \frac{\partial^2}{\partial x_i^2} + \sum_{\bar{\nu}} b_{\bar{\nu}}^{+} b_{\bar{\nu}} + i\left(\frac{4\pi\alpha}{S}\right)^{\frac{1}{2}} \sum_{\bar{\nu}} \frac{1}{\nu}\left(b_{\bar{\nu}}^{+} e^{-i\bar{\nu}\cdot\bar{x}} - b_{\bar{\nu}} e^{i\bar{\nu}\cdot\bar{x}}\right)$$

$$= F_0 + F_{int} \qquad (45)$$

where $F_0 \equiv \lim_{\alpha\to 0} F$. The perturbative approach proceeds by using the eigenstates of F_0 which are product functions of plane wave states and oscillator functions of the form

$$|\bar{k};\ n_{\bar{\nu}1},\ n_{\bar{\nu}2},\ \ldots,\ n_{\bar{\nu}},\ \ldots\rangle = S^{-\frac{1}{2}}\, e^{i\bar{q}\cdot\bar{x}} \prod\!\!\!\!\prod_{\bar{\nu}} |n_{\bar{\nu}}\rangle \quad . \qquad (46)$$

Here $\prod\!\!\!\!\prod_{\bar{\nu}}$ is the permutation operator symmetrizing $|n_{\bar{\nu}}\rangle$ and $\bar{k}$ is the total wave vector in dimensionless form of the plane wave and oscillators defined by

$$\bar{k} = \bar{q} + \sum_{\bar{\nu}} n_{\bar{\nu}}\, \bar{\nu} \quad . \qquad (47)$$

The energy eigenvalue of such a state in units of $\hbar\omega_L$ is

$$\varepsilon_0(\bar{k};\ \ldots,\ n_{\bar{\nu}},\ \ldots) = q^2 + \sum_{\bar{\nu}} n_{\bar{\nu}}$$

$$= [\bar{k} - \sum_{\bar{\nu}} n_{\bar{\nu}}\, \bar{\nu}]^2 + \sum_{\bar{\nu}} n_{\bar{\nu}} \quad . \qquad (48)$$

Provided the zero energy without any perturbation is less than $\hbar\omega_L$ ($n_{\bar{\nu}} = 0$), no degeneracies occur in the total wave vector $\bar{k}$ as given by Eq. (47) and straight forward perturbation theory may be applied. The ground state of F_0 is

$$|\bar{k};\ \ldots,\ 0_{\bar{\nu}},\ \ldots\rangle = S^{-\frac{1}{2}}\, e^{i\bar{k}\cdot\bar{x}}\, |0_{\bar{\nu}}\rangle \qquad (49)$$

with energy

$$\varepsilon_0(\bar{k};\ \ldots,\ 0_{\bar{v}},\ \ldots) = k^2 < 1 \ . \qquad (50)$$

In this representation there are no non-vanishing elements on the diagonal for F_{int}. The only non-zero elements are of the form

$$\langle \ldots,\ 0_{\bar{v}},\ \ldots;\ \bar{k}+\bar{v}\,|F_{int}|\,\bar{k};\ \ldots,\ 1_{\bar{v}},\ \ldots\rangle = \frac{i}{v}(4\pi\alpha/S)^{\frac{1}{2}} \ . \qquad (51)$$

From second order perturbation theory with Eqs. (48), (50), and (51)

$$E(k) = \hbar\omega_L[k^2-(4\pi\alpha/S)\sum_{\bar{v}} \frac{1/v^2}{(\bar{k}-\bar{v})^2 + 1 - \bar{k}^2}\ ] \qquad (52)$$

and transforming $\sum_{\bar{v}} \rightarrow S/(2\pi)^3 \int \ldots\ d^3\bar{v}$ gives an energy of

$$E(k) = \hbar\omega_L(k^2 - \alpha\ \frac{\sin^{-1}k}{k}\ )$$

$$\simeq \hbar\omega_L(k^2 - \alpha - \alpha k^2/6) \quad , \text{ for } k<1. \qquad (53)$$

When one defines the polaron mass, m_p, by the relationship

$$E(k) \equiv E(0) + (\hbar^2u^2/2m_p)\ k^2 + \ldots \quad , \qquad (54)$$

m_p may be solved for directly by using Eq. (43) and comparing Eqs. (53) and (54) to get

$$m_p = (1 + \alpha/6)\ m^* \ ; \quad \alpha<1. \qquad (55)$$

The second modification which may be made to describe more accurately this system is to include the possibility of an additional relaxation process at frequencies greater than

ω_L to account for more than the velocity dependent relaxation time τ in the Drude gas. The actual calculations are to be found in the paper by Gurevich, Lang, and Firsov[10] where a perturbative approach is taken for $\alpha<1$. Their results show that in addition to the usual zeroth order Drude term, there is a contribution to the imaginary part of the dielectric function for a second order process. The dissipation of electromagnetic energy described by

$$\varepsilon' = (8\pi Ne^2\alpha/3m^*\omega\omega_L)(\omega_L/\omega)^{\frac{5}{2}}(1-\omega_L/\omega)^{\frac{1}{2}} \qquad (56)$$

is a result of the process where an electron absorbs an infrared photon and simultaneously emits a longitudinal optical phonon of energy $\hbar\omega_L$. This contribution clearly vanishes when the frequency of the incident photon is less than that of the phonon.

If $\hbar\omega_L > kT$ which is the case in most materials at room temperature, then the process where a phonon is absorbed by the electron at the same time that a photon is absorbed is proportional to the number of these phonons already thermally excited. At room temperatures this process may be considered negligible to the absorption described by Eq. (56). However, as these phonons do become thermally excited, a noticeable temperature dependent absorption may be found in the reflectance curves for photon energies less than $\hbar\omega_L$ as suggested in Ref. 10.

Another process which might be examined by temperature

dependent measurements is the following. If a phonon of energy $\hbar\omega_L$ is emitted and a photon of energy $h\omega$ is absorbed, where now ω is less than ω_L, the energy lacking can be made up by the thermally excited electrons when $(\omega_L-\omega) < kT/\hbar$. Unfortunately this process would occur in the energy region where phonon processes are the determining factors for the reflectance spectrum. In Ref. 10 it is still suggested that the temperature dependence of this absorption would be apparent for $\omega < \omega_T$.

In the following curve fits, only the contribution of ε' is added the the dielectric function expressed by Eq. (22). It has the effect of increasing the imaginary part of the dielectric function from 2.43 to 2.80 where it has its maximum effect at $\omega = (8/7)\omega_L = 355\ cm^{-1}$.

In order to best fit the two polarizations, N had to be increased to $1.42 \times 10^{18}\ cm^{-3}$ due to the 10 percent increase in the effective mass from consideration of the polaron mass at frequencies less than ω_L. Also $1/\tau$ had to be decreased to $255\ cm^{-1}$. With no additional parameters, these two corrections produce the same fit everywhere except in the $300\ cm^{-1}$ to $600\ cm^{-1}$ range where the fit to the data is improved considerably as shown in Figs. 8 and 9. In this case where $\alpha<1$ the use of the perturbative approach in Ref. 10 for calculating the additional absorption as well as the polaron mass treatment in Ref. 9 are shown to be applicable.

This absorption was used in the case of $SrTiO_3$ by Barker[32] and found not to apply. A small polaron theory[33] was preferred.

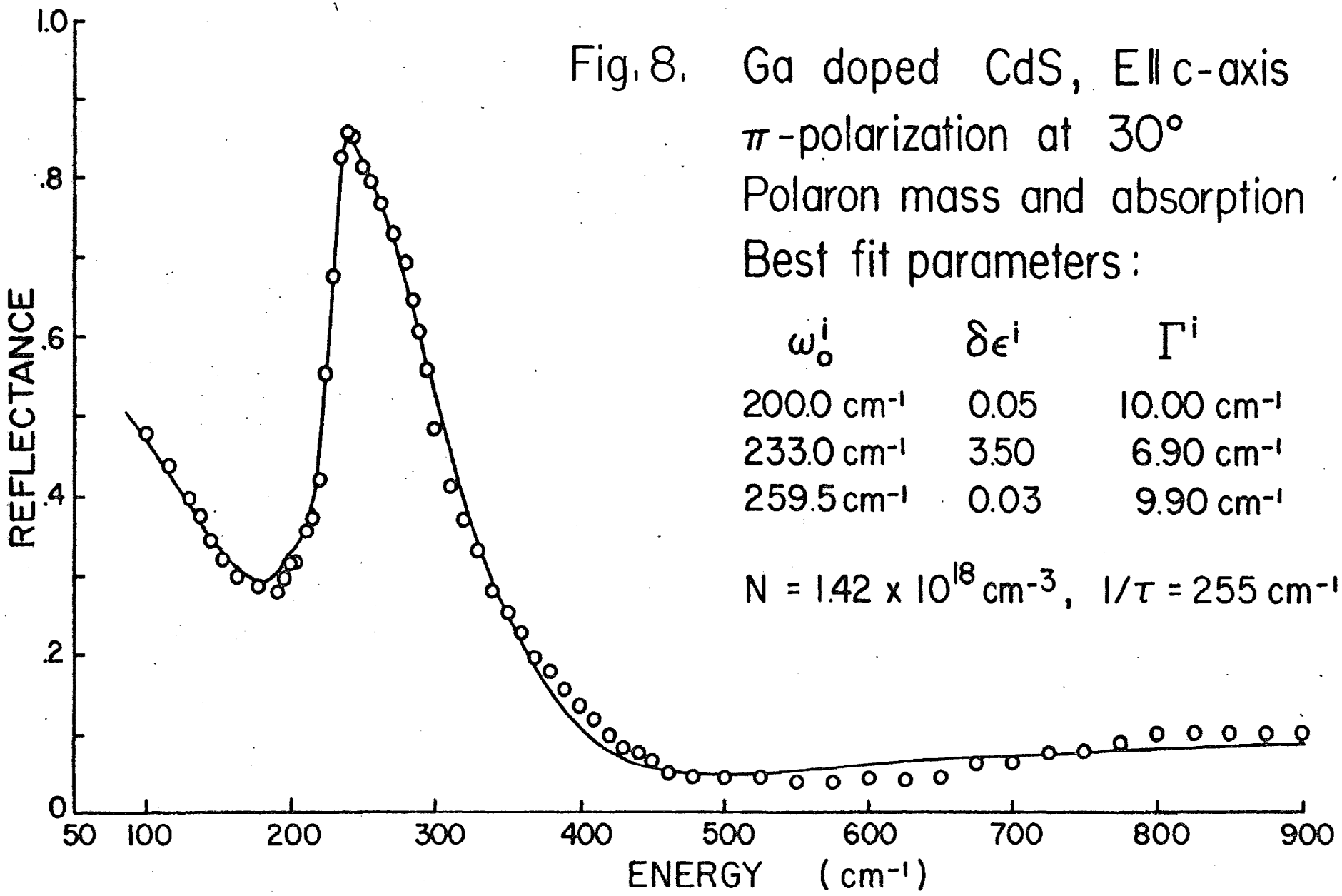

Fig. 8. Ga doped CdS, E ∥ c-axis
π-polarization at 30°
Polaron mass and absorption
Best fit parameters:

ω_o^i	$\delta\epsilon^i$	Γ^i
200.0 cm^{-1}	0.05	10.00 cm^{-1}
233.0 cm^{-1}	3.50	6.90 cm^{-1}
259.5 cm^{-1}	0.03	9.90 cm^{-1}

$N = 1.42 \times 10^{18}\ cm^{-3}$, $1/\tau = 255\ cm^{-1}$

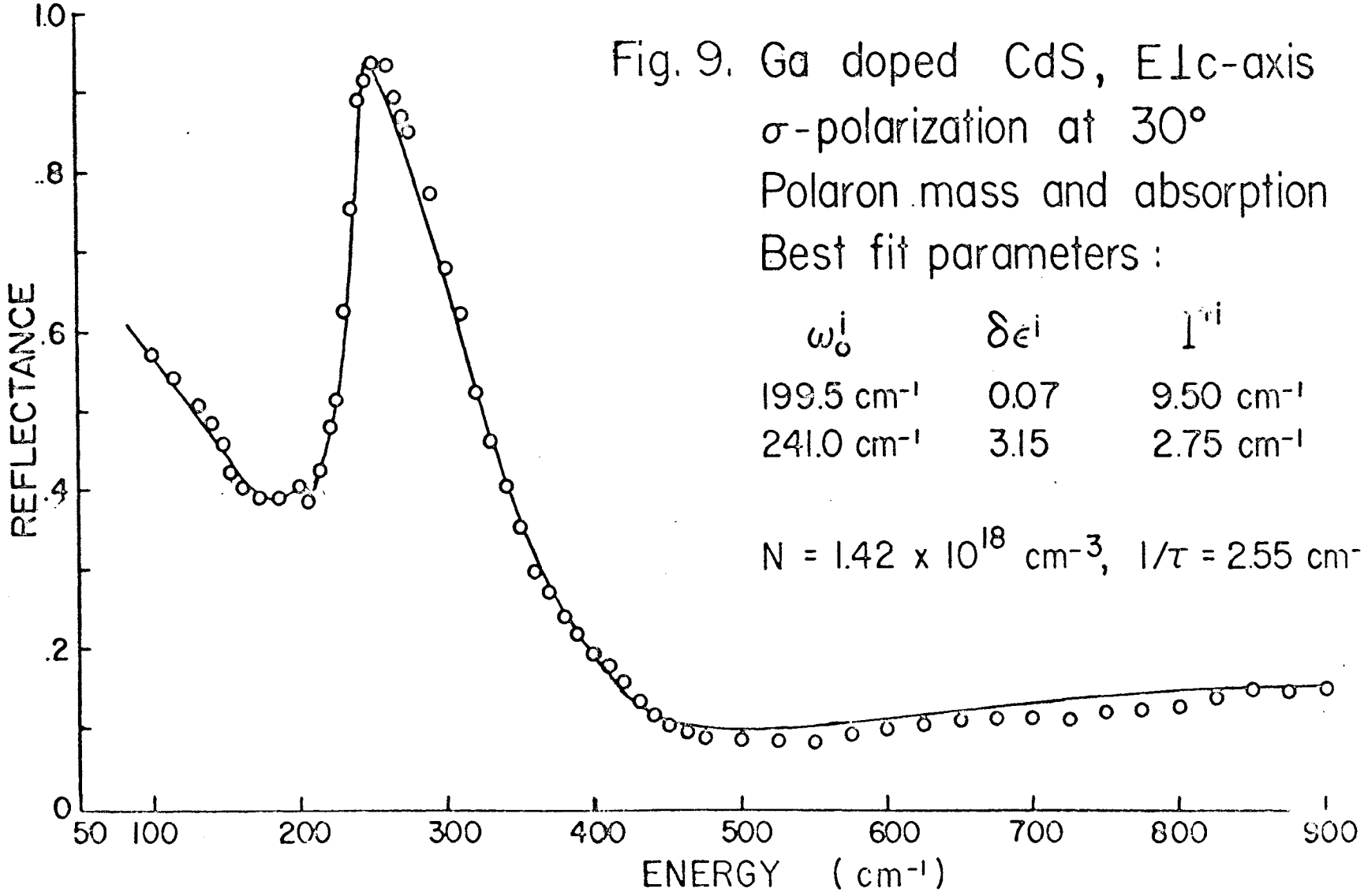

Fig. 9. Ga doped CdS, E⊥c-axis
σ-polarization at 30°
Polaron mass and absorption
Best fit parameters :

ω_o^i	$\delta\epsilon^i$	Γ^{ri}
199.5 cm^{-1}	0.07	9.50 cm^{-1}
241.0 cm^{-1}	3.15	2.75 cm^{-1}

$N = 1.42 \times 10^{18}$ cm^{-3}, $1/\tau = 2.55$ cm^{-1}

CHAPTER VIII

REFLECTANCE MINIMA

Without analysis of the mode frequencies, the most obvious change in the reflectance spectrum for the coupled system over the pure lattice system (provided the electron mobility is not too low) is the additional minimum below ω_o. Physically in pure, single mode ionic crystals such minima whose reflected fluxes approach zero occur at frequencies which are just those points on a dispersion plot where the free space photon curve crosses the coupled transverse optical phonon-photon curve as shown by point A in Fig. 10 below.

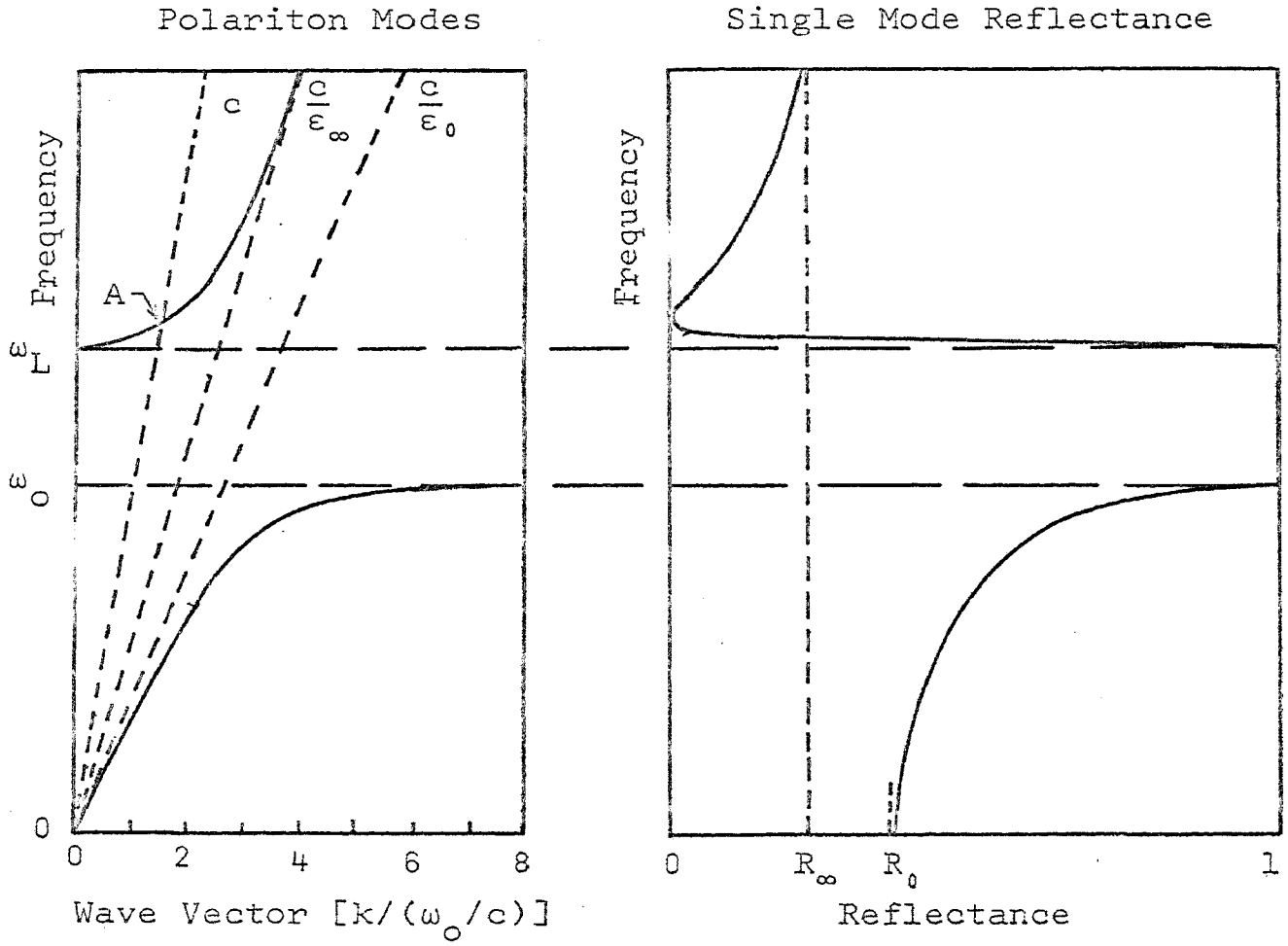

Fig. 10. Polariton modes and reflectance from a pure crystal.[24]

These coupled transverse modes in a solid are found from a complete solution of Eq. 28 and are usually referred to as polariton modes. Where these modes cross the free space photon curve, the transverse modes in free space and in the crystal have matching frequency and wave vector. The incident flux may then freely traverse the crystal and the reflectance is thus zero. At frequencies between $\omega_0=\omega_T$ and ω_L, $\varepsilon<0$ and there are no transverse solutions existing in the crystal when $\Gamma<<\omega_0$. The reflectance in this region is therefore unity.

At all other frequencies where transverse modes exist in the crystal, reflectance occurs in varying amounts depending on the amount of mis-match in the wave vector values of the modes in the crystal and in free space at a given frequency. The further the polariton wave vector is from the value of the photon wave vector at the frequency being considered, the greater is the reflectance value. The reflectance curve in Fig. 10 has been drawn using these ideas.

Arguments for the shape of the reflectance curve for the doped crystal are the same, but a dispersion plot includes more modes. These minima have been studied from the view point of Murray, et al.[39] in the case of CdS[40] but this fails as ω_P nears ω_L since the dielectric function in that work was composed of a frequency dependent plasma term and a frequency independent lattice term, i.e. no coupling. It may be seen in Ref. 40 where the coupling effects do become important in terms of free carrier concentration.

A more applicable relation including the coupling effects was derived later by using the physical properties of these minima. Stated in another way, these frequencies are the values at which $\varepsilon(0,\omega)$ is unity, i.e. the value of the free space dielectric constant. When absorption effects are negligible they are

$$\omega^2_{min} = \frac{\varepsilon_0(1+\omega_P^2/\omega_L^2)-1 \pm \{[\varepsilon_0(1+\omega_P^2/\omega_L^2)-1]^2-4\varepsilon_0(\varepsilon_\infty-1)\omega_P^2/\omega_L^2\}^{\frac{1}{2}}}{2(\varepsilon_\infty-1)/\omega_T^2} \quad . \quad (57)$$

At all concentrations Eq. (57) defines well the experimental minimum values for CdS and it works better when applied to the data for ZnO, GaAs, and InSb where the electron mobilities are higher. Figs. 11, 12, 13, and 14 show these results.

Just as in a description of the longitudinal mode frequencies plotted as a function of concentration, the lower branch of this minimum plot starts with complete plasma character where $\omega_P << \omega_L$. As ω_P approaches ω_L the lower curve becomes a result of the mixed plasma-phonon mode. Finally, as ω_P becomes much greater than ω_L the lower minimum's value is completely determined by the phonon frequency. A description of the upper branch of the minimum plot follows in a reverse manner.

Fig. 11. Reflectivity Minima for n-Type ZnO

—— ω_{MIN} from Varga dielectric function

o Collins and Kleinman (ref. 3)

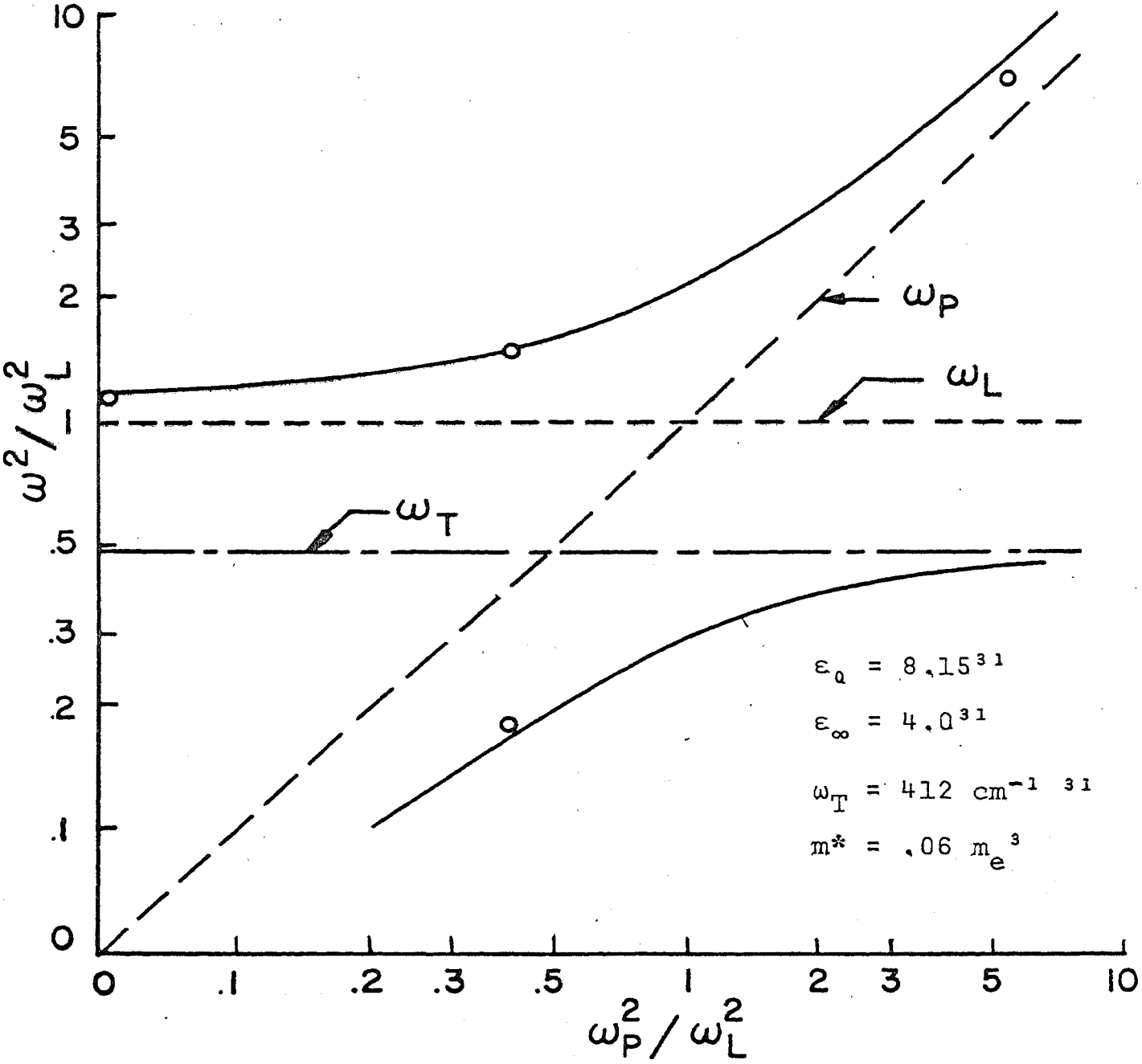

Fig.12. Reflectivity Minima for n-Type InSb

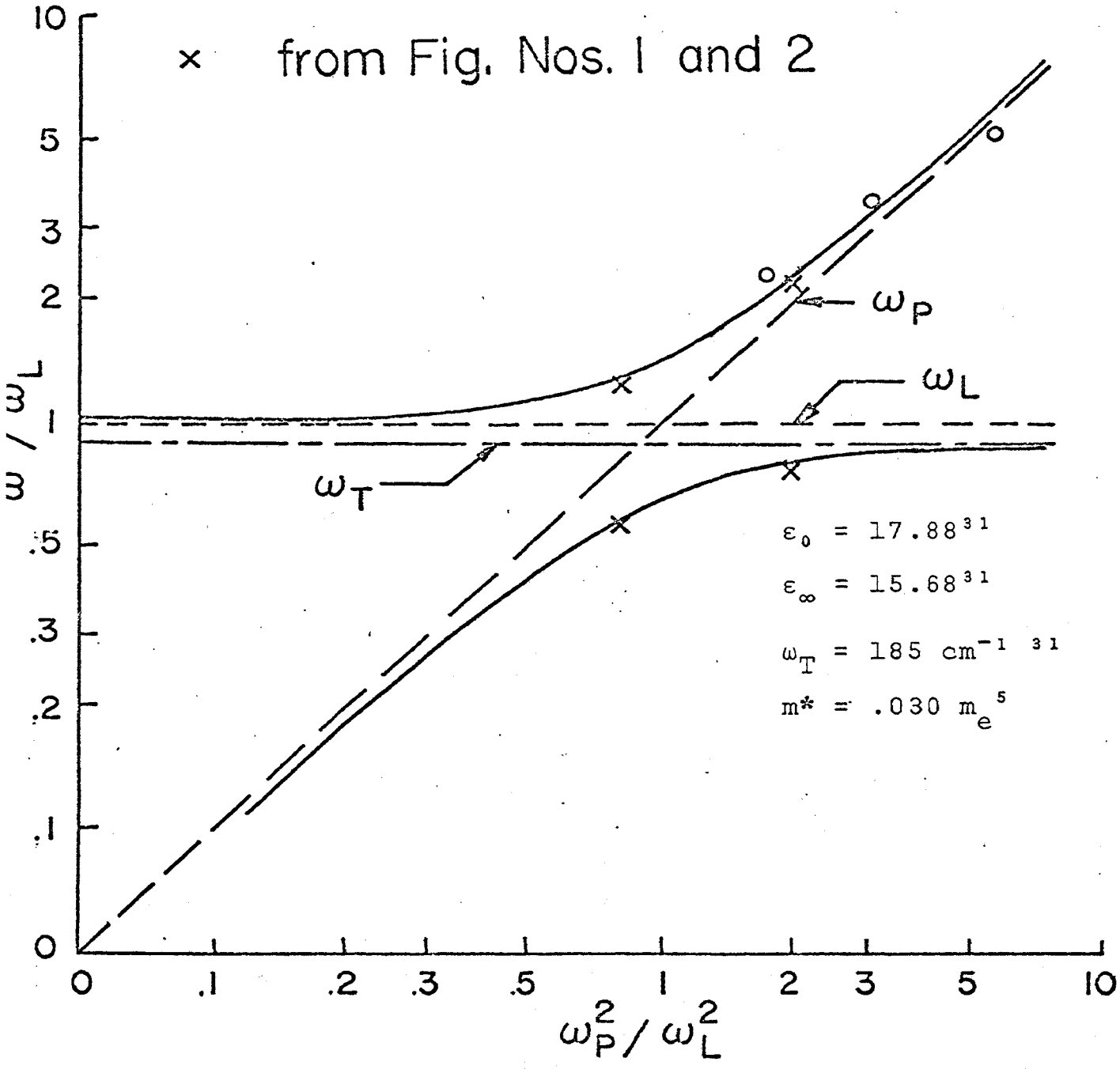

Fig.13. Reflectivity Minima for n-Type GaAs

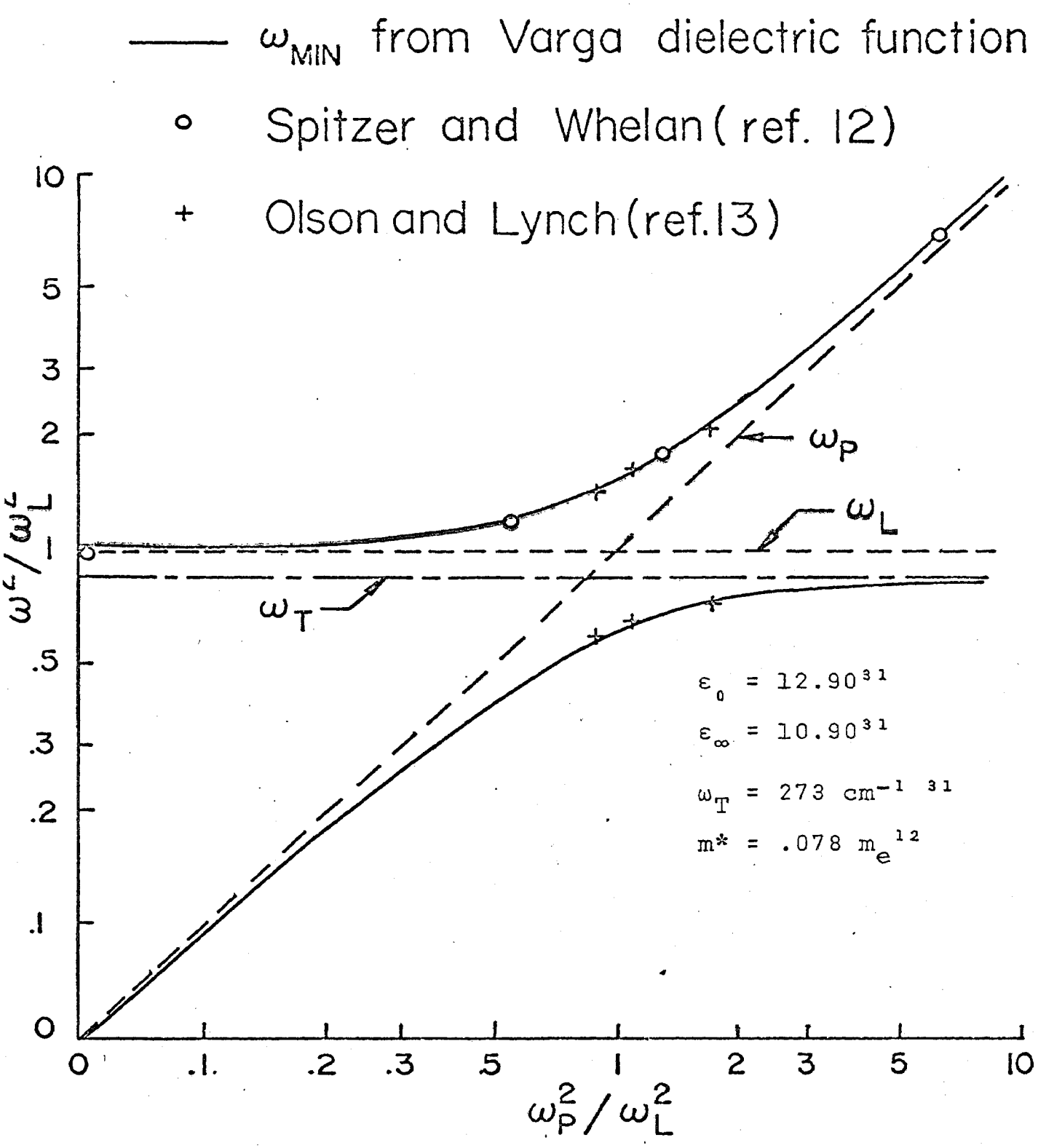

Fig.14. Reflectivity Minima for n- Type CdS

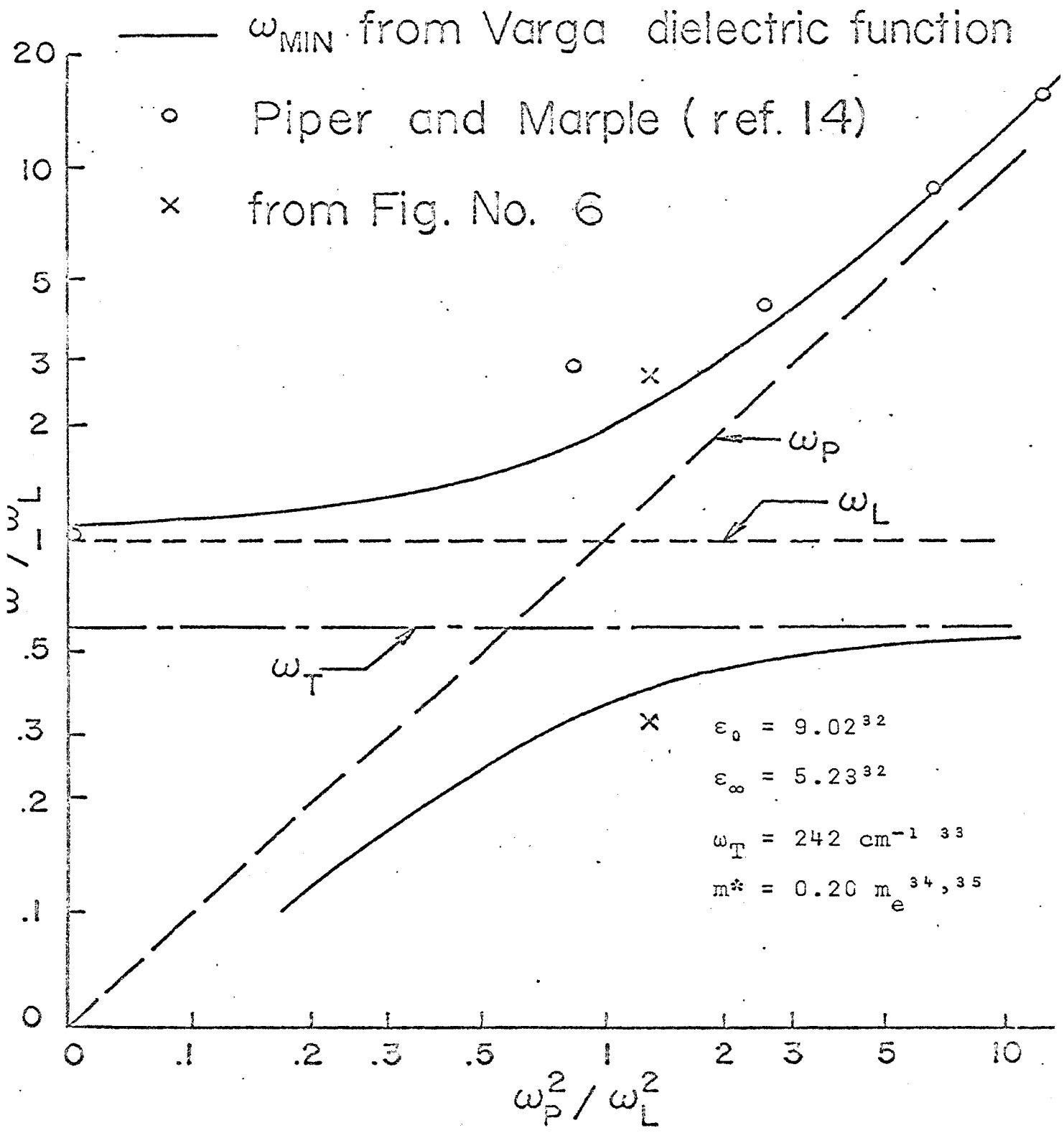

CHAPTER IX

SUMMARY

The accomplishments of this reflectance work may be placed in four main groups. First, the dielectric function derived by Varga[1] for the coupled system of free carriers and phonons has been shown to work well for the concentrations that would produce the maximum effect of this coupling at long wavelengths in both CdS and InSb. Second, the effective mass variation with concentration discussed by Spitzer and Fan[5] in InSb has been shown to occur because of the increased effect of this coupling as ω_P approaches ω_L. When this coupling is considered the effective mass varies only slightly.

Third, in CdS the change in effective mass of the free carriers due to the polarization of the lattice on passing to frequencies below ω_L has been shown to be consistant with the polaron theory of Fröhlich.[9] Fourth and last, the additional absorption which occurs in the plasma due to loss of energy to the longitudinal optical mode when $\omega>\omega_L$ in the approximation of Gurevich, et al.[10] can be considered to improve the reflectance fit in the case of CdS.

BIBLIOGRAPHY

1. B.B. Varga, Phys. Rev. 137, A 1896 (1965).

2. K.S. Singwi and M.P. Tosi, Phys. Rev. 147, 658 (1966).

3. R.J. Collins and D.A. Kleinman, J. Phys. Chem. Solids 11, 190 (1959).

4. A.S. Barker, Phys. Rev. 136, A 1290 (1964).

5. W.G. Spitzer and U.F. Fan, Phys. Rev. 106, 882 (1957).

6. A. Mooradian and G.B. Wright, Phys. Rev. Letters 16, 999 (1966).

7. A. Mooradian and A.L. McWhorter, Phys. Rev. Letters 19, 849 (1967).

8. B. Tell and R.J. Martin, Phys. Rev. 167, 381 (1968).

9. H. Frohlich, Advances in Physics 3, 325, (1954).

10. V.L. Gurevich, I.G. Lang, and Yu. A. Firsov, Sov. Phys. Sol. State 4, 918 (1962).

11. R.J. Bell, T.J. McMahon, and D.G. Rathbun, J. Appl. Phys. 39, 48 (1968).

12. W.C. Spitzer and J.M. Whelan, Phys. Rev. 114, 59 (1959).

13. C.G. Olson and D.W. Lynch, Phys. Rev. 177, 1231 (1969).

14. W.W. Piper and D.T.F. Marple, J. Appl. Phys. 32, 2237 (1961).

15. G.R. Bird and M.Parrish, Jr., J. Opt. Soc. Am. 50, 886 (1960).

16. J.W. Russell and H.L. Strauss, Appl. Opt. 4, 1131 (1965).

17. R.J. Bell and G.M. Goldman, J. Opt. Soc. Am. 57, 1552 (1967).

18. D.W. Berreman, Rev. Sci. Inst. 37, 513 (1966).

9. F.J. Low, J. Opt. Soc. Am. 51, 1300 (1961).

0. E.H. Putley and N. Shaw, "Comparison of the Detectivity of a Ge Bolometer With an InSb Sub-m.m. Detector", Royal Radar Establishment Memorandum 2115, Ministry of Aviation, Malvern, WORCS, England (Aug.1964).

1. A. Mitsuishi, Y. Yamada, H. Yoshinaga, J. Opt. Soc. Am. 52, 14 (1962).

2. R. Geick, Zeit. F. Physik 161 (1961).

3. A. Hadni, Essentials of Modern Physics Applied to the Study of the Infrared, (Pergamon Press, N.Y. (1967) p. 646).

4. M. Born and K. Huang, Dynamical Theory of Crystal Lattices, (Oxford at the Clarendon Press, London, 1954), Sections 8 and 9.

5. L.P. Mosteller, Jr., and F. Wooten, J. Opt. Soc. Am. 58, 511 (1968).

6. C.H. Henry and J.J. Hopfield, Phys. Rev. Letters 15, 964 (1965).

7. R.H. Lyddane, R.G. Sachs, and E. Teller, Phys. Rev. 59, 673 (1941).

8. A.S. Barker, Phys. Rev. 145, 391 (1966).

9. B. Szigeti, Trans. Faraday Soc. 45, 155 (1949).

0. T.S. Moss, Optical Properties of Semiconductors, Butterworths Scientific Publications, London, 224 (1959).

31. M.Hass and B.W. Henvis, J. Phys. Chem. Solids 23, 1099 (1962)

32. L.R. Shiozawa, et al., "Research on II-VI Compound Semiconductors," 9th Quarterly Progress Report, Contract No.AAF 33(651)-7399, U.S.A.F. Aerospace Research Laboratory, Wright-Patterson A.F.B.

33. H.W. Verleur and A.S. Barker, Jr., Phys. Rev. 155, 750 (1967).

34. A. Misu, K. Aoyagi, G. Kuwabara, and S. Sugano, *International Conference on Semiconductors, Paris* (Academic Press Inc., Ner York, 1964), P. 317.

35. J.J. Hopfield and D.G. Thomas, Phys. Rev. 119, 570 (1960).

36. T.D. Lee, F.E. Low, and D. Pines , Phys, Rev. 90, 297 (1953).

37. A.S. Barker, Jr., Optical Properties and Electronic Structure of Metals and Alloys, (North Holland Publishing Co., Amsterdam, 1966).

38. H.G. Reik, E. Kauer, P. Gerthsen, Phys. Letters 8, 29 (1964).

39. L.A. Murray, J.J. Rivera, and P.A. Hass, J. Appl. Phys. 37, 4743 (1966).

40. R.J. Bell, Phys. Letters 24A, 576 (1967).

APPENDIX

Computer program for the tabulation and plotting of the off normal incidence reflectances R_π and R_σ, real part of $\varepsilon(0,\omega)$, and imaginary part of $\varepsilon(0,\omega)$ with or without the polaron mass and absorption as a function of frequency.

```
DIMENSION C8(200),C9(200),C8P(200),C9P(200)
CALL PENPOS('MCMAHON,THOMAS',14,0)
CALL NEWPLT(2.0,3.5,12.0)
CALL ORIGIN( 0.0,0.00)
CALL XSCALE(0.0,900.0,9.0)
CALL YSCALE(0.00,1.00,5.00)
REAL MSP,MSD
THETA=30.0/57.296
C=3.E+10
PI=3.1416
QE=4.803E-10
SME=0.2*(9.11E-28)
EI=5.17
ALPHA=0.58
WT=199.5
WT1=241.0
WT2=258.0
G=9.50
G1=2.75
G2=9.0
TI=255
DEP=0.07
DEP1=3.15
DEP2=0.0
ON=1.42E+18
W=5.0
WL1=(SQRT((EI+DEP1)/EI))*WT1
MSP=SME
IF(W.LT.WL1) MSP=SME*(1+ALPHA/6)
WP=(SQRT((4.*PI*ON*QE**2)/(1.0*MSP*EI)))/(2.*PI*C)
QP=(SQRT((4.*PI*ON*QE**2)/(1.0*SME*EI)))/(2.*PI*C)
DW=5.0
EIP=5.23
ALPHP=0.58
WTP=200.0
WT1P=233.0
WT2P=259.5
GP=10.0
G1P=6.90
G2P=9.00
DEPP=0.05
DEP1P=3.50
DEP2P=0.025
WL1P=(SQRT((EIP+DEP1P)/EIP))*WT1P
MSD=SME
IF(W.LT.WL1P) MSD=SME*(1+ALPHP/6)
WPP=(SQRT((4.*PI*ON*QE**2)/(1.0*MSD*EIP)))/(2.*PI*C)
QPP=(SQRT((4.*PI*ON*QE**2)/(1.0*SME*EIP)))/(2.*PI*C)
WRITE(3,100) WP,ON,WPP
WRITE (3,99)
```

```
      DO 1 I=1,180,1
      C1=1.-(W/WT)**2
      C2=W*G/WT**2
      C3=1.-(W/WT1)**2
      C4=W*G1/WT1**2
      C5=1.-(W/WT2)**2
      C6=W*G2/WT2**2
      C12=DEP/(C1**2+C2**2)
      C34=DEP1/(C3**2+C4**2)
      C56=DEP2/(C5**2+C6**2)
      C78=(EI*(WP**2)*W)/(W**4+(W*TI)**2)
      C8(I)=EI+C1*C12+C3*C34+C5*C56-W*C78
      C9(I)=C78*TI+C2*C12+C4*C34+C6*C56
      IF(W.GT.WL1) C9(I)=C9(I)+2*(QP**2)*EI*ALPHA*(SQRT(((WL1/W)**5)*(1.
     1-WL1/W)))/(WL1*W*3)
      AN=SQRT(C8(I)/2.+(SQRT(C8(I)**2+C9(I)**2))/2.)
      AK=C9(I)/(2.*AN)
      CALL RSIGMA(AN,AK,THETA,RA)
      CALL XYPLT(W,PA,1,2,1)
      C1P=1.-(W/WTP)**2
      C2P=W*GP/WTP**2
      C3P=1.-(W/WT1P)**2
      C4P=W*G1P/WT1P**2
      C5P=1.-(W/WT2P)**2
      C6P=W*G2P/WT2P**2
      C12P=DEPP/(C1P**2+C2P**2)
      C34P=DEP1P/(C3P**2+C4P**2)
      C56P=DEP2P/(C5P**2+C6P**2)
      C78P=(EIP*(WPP**2)*W)/(W**4+(W*TI)**2)
      C8P(I)=EIP+C1P*C12P+C3P*C34P+C5P*C56P-W*C78P
      C9P(I)=C78P*TI+C2P*C12P+C4P*C34P+C6P*C56P
      IF(W.GT.WL1P) C9P(I)=C9P(I)+2*(QPP**2)*EIP*ALPHP*(SQRT(((WL1P/W)**
     25)*(1-WL1P/W)))/(WL1P*W*3)
      ANP=SQRT(C8P(I)/2.+(SQRT(C8P(I)**2+C9P(I)**2))/2.0)
      AKP=C9P(I)/(2.*ANP)
      CAP=AN*ANP-AK*AKP
      DAP=AN*AKP+ANP*AK
      CALL RPIE(AN,AK,THETA,CAP,DAP,RAP)
      CALL XYPLT(W,RAP,1,2,5)
      WRITE(3,301) W,C8(I),C9(I),RA,C8P(I),C9P(I),RAP
      W=W+DW
    1 CONTINUE
      CALL YAXIS(0.05)
      CALL XAXIS(10.0)
      CALL ENDPLT
      CALL NEWPLT(0.0,3.5,12.0)
      CALL ORIGIN(0.0,0.0)
      CALL TSCALE(0.0,180.0,9.0)
      CALL YSCALE(-90.0,190.0,6.00)
      CALL TAXIS(2.0)
      CALL YAXIS(10.0)
      CALL TPLT(C8 ,181,2,1)
      CALL NEWPLT(0.0,3.5,12.0)
      CALL ORIGIN(0.0,0.0)
      CALL TSCALE(0.0,180.0,9.0)
      CALL YSCALE(-90.0,190.0,6.00)
      CALL TAXIS(2.0)
      CALL YAXIS(10.0)
      CALL TPLT(C9 ,181,2,1)
      CALL ENDPLT
```

```
      CALL NEWPLT(0.0,3.5,12.0)
      CALL ORIGIN(0.0,0.0)
      CALL TSCALE(0.0,180.0,9.0)
      CALL YSCALE(-90.0,190.0,6.00)
      CALL TAXIS(2.0)
      CALL YAXIS(10.0)
      CALL TPLT(C8P,181,2,1)
      CALL NEWPLT(0.0,3.5,12.0)
      CALL ORIGIN(0.0,0.0)
      CALL TSCALE(0.0,180.0,9.0)
      CALL YSCALE(-90.0,190.0,6.00)
      CALL TAXIS(2.0)
      CALL YAXIS(10.0)
      CALL TPLT(C9P,181,2,5)
      CALL ENDPLT
      CALL LSTPLT
      CALL EXIT
   99 FORMAT(7X,'W',9X,'N*N-K*K',8X,'2*N*K',9X,'RSIGMA',6X,'NP*NP-NK*NK'
     1,6X,'2*NP*NK',11X,'RPIE')
  100 FORMAT(4X,'WP= ',F10.2,10X,'CONCENTRATION= ',F10.4,10X,'WPP= ',F10
     8.2,//)
  301 FORMAT(4X,F7.2,6X,F8.4,6X,F8.4,6X,F11.8,6X,F8.4,6X,F8.4,6X,F11.8)
      END
```

```
      SUBROUTINE RSIGMA(AN,AK,THETA,RSIG)
      FIRST=AN**2-AK**2-(SIN(THETA))**2
      SECOND=SQRT((FIRST**2)+4.0*(AN**2)*(AK**2))
      TOUSQD=FIRST+SECOND
      TOVSQD=SECOND-FIRST
      U=(1.0/1.414)*SQRT(TOUSQD)
    2 V=(1.0/1.414)*SQRT(TOVSQD)
      RSIG=((COS(THETA)-U)**2+V**2)/((COS(THETA)+U)**2+V**2)
      RETURN
      END
```

```
      SUBROUTINE RPIE(AN,AK,THETA,CAP,DAP,RPI)
      FIRSP=AN**2-AK**2-(SIN(THETA))**2
      SECONP=SQRT((FIRSP**2)+4.0*(AN**2)*(AK**2))
      TOUSQP=FIRSP+SECONP
      TOVSQP=SECONP-FIRSP
      UP=(1.0/1.414)*SQRT(TOUSQP)
      VP=(1.0/1.414)*SQRT(TOVSQP)
      RPI=((CAP*COS(THETA)-UP)**2+(DAP*COS(THETA)-VP)**2)/((CAP*COS(
     8THETA)+UP)**2+(DAP*COS(THETA)+VP)**2)
      RETURN
      END
```

VITA

The author, Thomas Joseph McMahon, was born on December 27, 1943, in Rahway, New Jersey. He received his primary and secondary education in Elmhurst, Illinois. He received a Bachelor of Science Degree in Engineering Physics and a Master of Science Degree in Physics from the University of Illinois in Urbana, Illinois in February 1965 and June 1966, respectively.

He has been enrolled in the Graduate School of the University of Missouri - Rolla since June, 1966 and has held a U.S. Bureau of Mines Fellowship from that time through the completion of his Doctor of Philosophy Dissertation.